arXiv:nucl-th/0306071v2 9 Jul 2003

TOPICAL REVIEW

Reaction models to probe the structure of light exotic nuclei

Jim Al-Khalili[1] **and Filomena Nunes**[2]

[1)]School of Electronics and Physical Sciences, University of Surrey, Guildford, GU2 7XH, U.K.

[2)]National Superconducting Cyclotron Laboratory, Michigan State University, East Lansing, Michigan 48824, USA

Abstract. We review here theoretical models for describing various types of reactions involving light nuclei on the driplines. Structure features to be extracted from the analysis of such reaction data, as well as those that need to be incorporated in the reaction models for an adequate description of the processes, are also under focus. The major unsolved theoretical issues are discussed, along with some suggestions for future directions of the field.

1. Introduction

A number of experimental reviews on the physics of light exotic nuclei [1, 2, 3] have focused mainly on experimental techniques and the physics that could be extracted from those measurements. Any attention paid to the reaction models used in the analyses was rather modest, and has appeared mainly in conference proceedings [4, 5, 6, 7]. Our aim in this paper is to fill this gap by reviewing the progress in the theory of modelling reactions with light dripline nuclei.

In the early days of our field, total reaction cross section measurements were used to obtain information on halo nuclei. This observable was one of the key pieces of evidence for the extended density tails (large matter radii [8, 9]). However, depending on the reaction model used, results could differ significantly: if the appropriate granular structure of the projectile was included in the reaction model [10], one concluded, from the same data, that halo nuclei were much larger than predicted using one-body density models.

This is the first of many examples where there is an interplay between structure and reaction. As the properties of these exotic nuclei became evident (see figure (1)), reaction models were modified in order to incorporate the essential known structure features. The essence of these features could be summarised as:

(i) finite range effects extending out farther than expected, due to the very long tails of the wavefunctions;

(ii) strong recoil effects due to the few-body granular structure;

(iii) continuum effects due to the proximity to threshold.

The numerous cases discussed in this review are an illustration of the importance of including these ingredients in the reaction model.

Following total reaction cross section data, and as soon as the beam intensity allowed, elastic scattering for many of these nuclei was measured, raising some paradigmatic questions about the type of optical potentials required to fit the angular distributions that are still not satisfactorily answered. However, it was the study of breakup observables that attracted most of the theoretical effort. Starting with momentum distributions, which essentially confirmed the large spatial extension of the valence nucleons, progress lead to experiments with complete kinematics, producing good quality angular and energy distributions of the fragments.

Technical developments, both in the detection system and beam production, enabled not only experiments with a larger variety of exotic nuclei but, more importantly, measurements of the traditional transfer and fusion reactions, the basis of most of the knowledge on stable nuclei. Consequently, systematic measurements of knock-out and transfer reactions, gave way to further theoretical developments. The puzzling reports from recent fusion measurements are presently a strong motivation for advances in the theory of fusion reactions.

Most of the reaction theory for light nuclei on the driplines has been developed

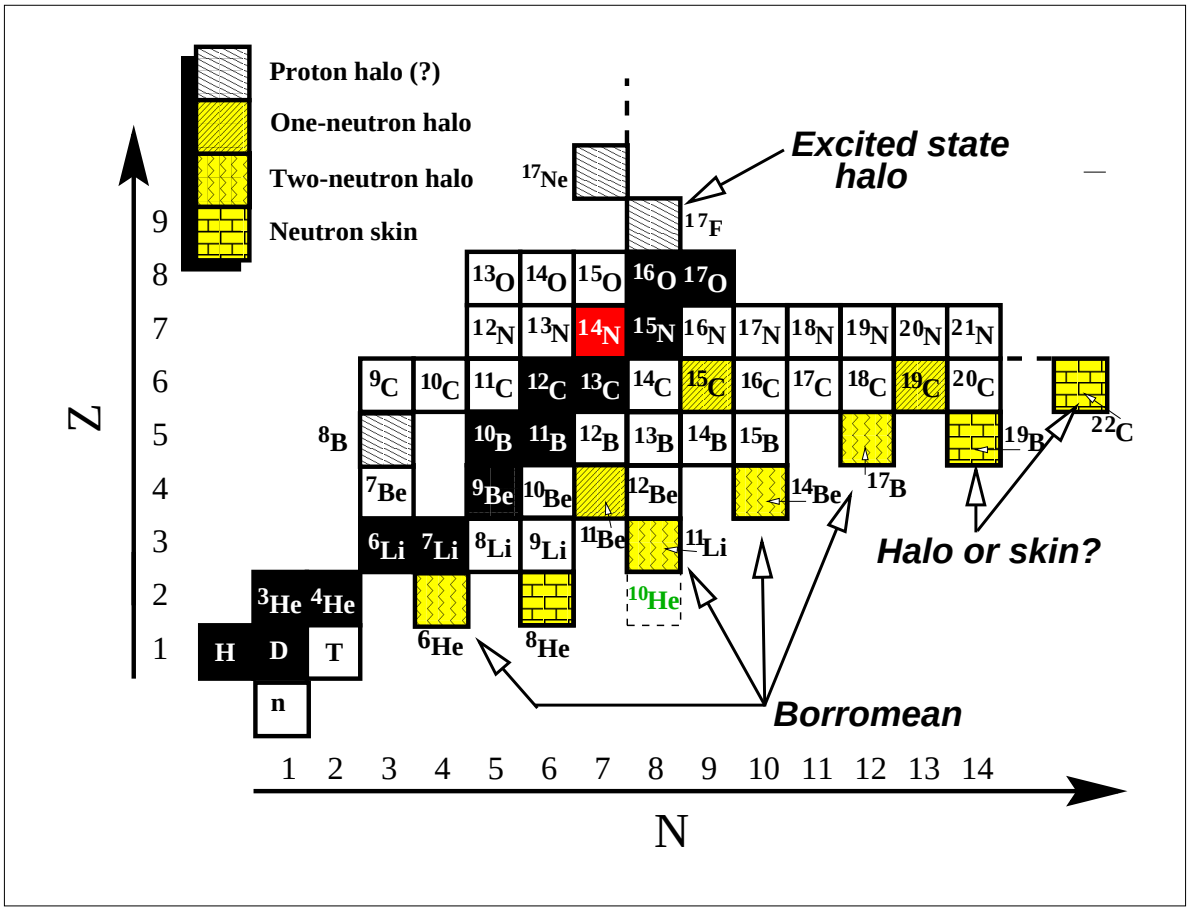


Figure 1. The light end of the chart of nuclides showing where much of the current interest has been focused. Some of the dripline nuclides found to exhibit new phenomena, such as halos, are highlighted.

for the high energy regime of fragmentation beams where convenient approximations can be made. These include the eikonal approximation, the adiabatic or *frozen halo* approximation, first order perturbation theory, or even isolating the nuclear and Coulomb transition amplitudes and treating them in different ways. Fortunately, fragmentation data has been abundant, providing crucial checks, allowing the identification of the exotic features that need to be assimilated. Looking through the past two decades, it is fair to say that significant progress has been made and that it has been predominantly through the analysis of these high energy data that we have learnt what we know about light dripline nuclei.

In our view, a new era is beginning. We are no longer trying to learn general features but the detailed structure. Unquestionably, it is harder to model reactions at low energy. The adiabatic and eikonal simplifications are no longer expected to hold, couplings are usually more important and isolating the nuclear and Coulomb parts is often not possible. However, low energy data contain more detailed information on the structure. The history of stable nuclear physics shows that most of the detailed

knowledge came from low energy data. The large number of new generation ISOL facilities that have or will become operational (e.g. SPIRAL-GANIL, REX-ISOLDE, EXCYT, MAFF, ISAC-TRIUMF, HRIBF(Oak-Ridge), RIA-ANL, E-arena(JHF)) will ensure progress in this direction.

In this review we report on both high energy and low energy reactions models. Section 2 examines the theoretical tools of various useful methods. Here we discuss the basic ideas behind each method, summarising the formalism and providing the relevant references. In Section 3, the models for analysis of total reaction cross sections are presented. In section 4, elastic and inelastic scattering studies are considered. Section 5 will cover the range of breakup models presently in use, from the coupled channels CDCC method to the traditional DWBA, including time dependent, semiclassical approaches as well as the models for high energy reactions, mostly applied to momentum distributions. In Section 6, the model used to analyze knock-out data is discussed, followed by a discussion of the applications of transfer reactions to extract structure information (Section 7). In Section 8, we give an account of the present status of fusion models. In section 9 we look at the modeling of other types of reactions which do not fit in any of the previous sections. Finally, in Section 10, we conclude with a discussion on some of the main open issues that need to be tackled in the near future, including theoretical considerations for reactions with electron beams.

2. Theoretical tools

In this section we give a brief outline of several approaches for calculating reaction observables for light exotic nuclei. The common feature of these systems is their weak binding and few-body nature. It is often therefore important to treat their reactions within few-body models also. We thus begin by discussing a number of theoretical techniques which provide approximate descriptions of the scattering and reactions of composite nuclei over a wide range of incident energies.

2.1. Few-body model space

In general, we require approximate solutions of the time-independent few-body Schrödinger equation. In this review, we focus mainly on projectiles which, to a good approximation, can be described as strongly-correlated n-body systems, where the n constituents can be individual nucleons or more massive clusters of many nucleons. The projectile's ground state is assumed to be a bound state, $\phi_0^{(n)}$ of the n constituents, each of which can interact with a target nucleus via complex two-body effective interaction, V_{jT}. This potential is identified with the energy-dependent phenomenological optical potential obtained by fitting reaction data for the $j + T$ binary system at the same incident energy per nucleon as the full projectile. If such data are not available then these potentials are calculated, either from folding models or, more microscopically, from multiple scattering theory.

In most cases of interest, the projectile nucleus has only one or two particle stable bound states, which couple strongly to the continuum during the reaction process. A major feature of few-body reaction models is therefore the inclusion of such projectile breakup effects in the reaction theory.

The Schrödinger equation satisfied by the scattering wavefunction of the effective $(n+1)$-body (projectile and target) system, $\Psi^{(+)}$, when the projectile is incident with wave vector $\vec{K}_0$ in the cm frame, is

$$[\,H\,-\,E]\,\Psi^{(+)}_{\vec{K}_0}(\vec{R},\vec{r}_1,\cdots,\vec{r}_n)=0\quad , \tag{1}$$

with total Hamiltonian $H = T_R + U(\vec{R}_1,\cdots,\vec{R}_n) + H_p$. Here H_p is the internal Hamiltonian for the projectile and T_R is the projectile cm kinetic energy operator. The vectors $\{\vec{r}_i\}$ are the relative (internal) coordinates between the projectile constituents, and $\{\vec{R}_j\}$ are the position vectors of the projectile constituents with respect to the target (see figure (2)). The total interaction between the projectile and target is just the sum of projectile constituent-target interactions:

$$U(\vec{R}_1,\cdots,\vec{R}_n)=\sum_{j=1}^{n}V_{jT}(R_j)\ . \tag{2}$$

The n-body projectile ground state wavefunction $\phi_0^{(n)}$ satisfies

$$H_p\,\phi_0^{(n)}(\vec{r}_1,\cdots,\vec{r}_n)=-\varepsilon_0\,\phi_0^{(n)}(\vec{r}_1,\cdots,\vec{r}_n)\ . \tag{3}$$

H_p will also generate an excited continuum spectrum and may support a finite number of bound or resonant excited states. We thus seek solutions of the few-body scattering wave function $\Psi^{(+)}_{\vec{K}_0}$ which satisfy the scattering boundary conditions

$$\Psi^{(+)}_{\vec{K}_0}=e^{i\vec{K}_0\cdot\vec{R}}\,\phi_0^{(n)}\ +\ \text{outgoing waves}\quad , \tag{4}$$

and where the target nucleus is assumed to remain in its ground state. For a projectile with a single bound state, the outgoing waves include only elastic scattering and elastic break-up channels. More generally, the outgoing waves will also include terms from any inelastically excited bound states.

It is implicit in the following that the methods we discuss yield only approximate solutions of the physical n-body problem. In particular one- and multi-constituent rearrangement channels are absent in the asymptotic ($R\to\infty$) regions of the derived solutions, due to our use of complex constituent-target interactions and radial and orbital angular momentum truncations[12]. In fact, all the theoretical schemes calculate approximations to $\Psi^{(+)}$ which are expected to be accurate representations of the n-body dynamics only within a restricted volume of the configuration space, or within a given interaction region. Reaction or scattering amplitudes can nevertheless be calculated reliably by using the wavefunction within an appropriate transition matrix element.

2.2. Continuum discretisation method

The most accurate theoretical technique available for reactions involving a projectile that can be reliably modeled as a two-cluster system is the method of coupled discretised

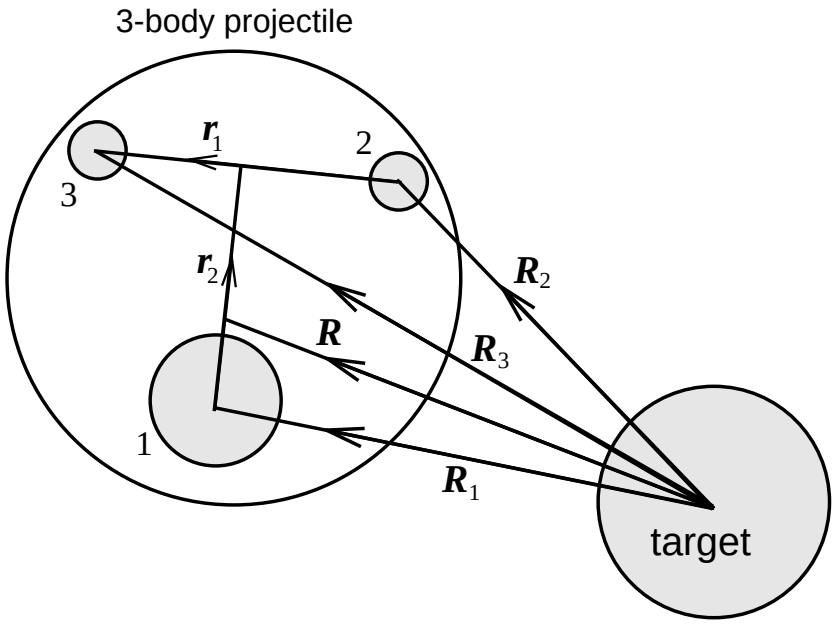


Figure 2. Definition of the coordinate vectors used in the case of the scattering of a three-body projectile from a target.

continuum channels (CDCC) [12]. It was originally formulated and applied to the scattering of the deuteron (n+p), ^{6}Li (α+d) and ^{7}Li (α+t), but has more recently been applied to a number of loosely-bound core+valence nucleon modeled dripline nuclei. The method cannot, however, be extended readily to three-body projectiles, such as the Borromean nuclei (^{6}He and ^{11}Li), although progress in developing such a four-body CDCC model is being made.

The CDCC method approximates the three-body Schrödinger equation as a set of effective two-body coupled-channel equations by constructing a square integrable basis set $\{\phi_\alpha\}$ of relative motion states between the two constituents of the projectile (including as well as the bound states, a representation of the continuum).

Projectiles treated using the CDCC method tend to have very few (often just one) bound states and the method provides a means of describing excitations to the continuum. Each of the physically significant set of spin-parity relative motion excitations is divided (or 'binned') into a discrete set of energy or momentum intervals up to some maximum value.

The CDCC method therefore works with the model space Hamiltonian

$$H^{CDCC} = PHP, \qquad P = \sum_{\alpha=0}^{N} |\phi_\alpha\rangle\langle\phi_\alpha|, \tag{5}$$

where the subscript α refers to the set of discrete states (ground state plus excited states) corresponding to energy eigenvalues $\varepsilon_\alpha = \langle\phi_\alpha|H_p|\phi_\alpha\rangle$. The corresponding asymptotic wavenumbers K_α, associated with the cm motion of the projectile in these excited

configurations, are such that

$$\hbar^2 K_\alpha^2/2\mu_p + \varepsilon_\alpha = \hbar^2 K_0^2/2\mu_p - \varepsilon_0 = E \ . \tag{6}$$

These bin states, together with the ground state, constitute an $(N{+}1)$ state coupled-channels problem for solution of the CDCC approximation to $\Psi^{(+)}$

$$\Psi^{CDCC}_{\vec{K}_0}(\vec{r},\vec{R}) = \sum_{\alpha=0}^{N} \phi_\alpha(\vec{r})\chi_\alpha(\vec{R}), \tag{7}$$

where $\alpha = 0$ refers to the projectile ground state. Explicitly

$$\left[T_R \ + \ V_{\alpha\alpha}(\vec{R}) \ - \ E_\alpha \right] \chi_\alpha(\vec{R}) = - \sum_{\beta\neq\alpha} V_{\alpha\beta}(\vec{R})\chi_\beta(\vec{R}), \tag{8}$$

with $E_\alpha = E - \varepsilon_\alpha$. The coupling interactions are

$$V_{\alpha\beta}(\vec{R}) = \langle \phi_\alpha | U(\vec{R}_1, \vec{R}_2) | \phi_\beta \rangle, \tag{9}$$

keeping in mind the definition of $\vec{R}$, $\vec{R}_1$ and $\vec{R}_2$ as illustrated in figure (2).

The evaluation of these couplings involves additional practical truncations of the CDCC model space, namely of *a*) the maximum order used in the multipole expansion of the interactions U, and *b*) the maximum radius r_{bin} used in evaluating these matrix elements. These must be chosen to be consistent with the included J_p^* channels, the bin widths Δk_i and interaction ranges.

Convergence of the calculations are then tested for different sizes of this model space. The number of bins and their upper limit depend on the particular state they are describing. The parameters must of course be carefully chosen to map any characteristic or resonant features in the projectile continuum. The different schemes for construction of the bin states are discussed extensively in the literature [13].

Solution of the coupled equations is carried out by usual partial wave decomposition. This allows the calculation of the elastic or inelastic scattering amplitude required for observables such as the differential cross section angular distribution. The CDCC scheme is available in a general coupled-channels computer code [14, 15].

Nuclear and Coulomb breakup of two-body projectiles, such as ^{8}B, ^{11}Be, ^{17}F and ^{19}C, can also be calculated with this model. The breakup transition amplitudes $T_m(\vec{k},\vec{K})$ from an initial state J, m to a general physical three-body final state of the constituents, with final state cm wave vector $\vec{K}$ and relative motion wave vector $\vec{k}$, is done by replacing Ψ^{CDCC} in an exact post-form matrix element [16],

$$T_m(\vec{k},\vec{K}) = \langle \phi^{(-)}_{\vec{k}}(\vec{r})\, e^{i\vec{K}\cdot\vec{R}} | U | \Psi^{CDCC}_{\vec{K}_0 m}(\vec{r},\vec{R}) \rangle \quad . \tag{10}$$

Inserting the set of bin-states, assumed complete for the model space used, then allows us to write the transition amplitude as a sum of amplitudes for each bin state, calculated by solving the coupled equations [13].

2.3. Adiabatic (sudden) approximation

For reactions involving incident projectile energies above a few tens of MeV per nucleon, a considerable simplification to the CDCC method can be applied if we make use of an

adiabatic treatment of the dynamics. By identifying the energetic (fast) variable with the projectile's cm motion coordinate, $\vec{R}$, and the slow variable with the projectile's internal coordinates, $\vec{r}_i$, the few-body Schrödinger equation can be reduced to a much simpler two-body form where the dynamical variable is only $\vec{R}$ and the projectile's internal degrees of freedom enter only as parameters (to be integrated over later). In the model, as formulated by Johnson and Soper [17], the approximation amounts to assuming that the breakup energies ε_k associated with the most strongly coupled excitation configurations in equation (1) are such that $\varepsilon_k \ll E$. Equivalently, due to the slow internal motions of the constituents of the projectile, the $\{\vec{r}_i\}$ are assumed frozen for the time taken for the projectile to traverse the interaction region. This approximation is also the starting point for the few-body Glauber method, based on impact parameter descriptions, discussed in the next subsection.

The crucial step is to replace H_p by $-\varepsilon_0$, the projectile ground state binding energy. This is done to satisfy the incident channel boundary conditions (the projectile is incident in its ground state). What has been assumed here is that, while the projectile does couple to excited and breakup states, they are all taken to be degenerate with the energy of the dominant elastic channel, ε_0. The adiabatic Schrödinger equation is therefore, with $E_0 = E + \varepsilon_0$,

$$[\,T_R \,+\, U \,-\, E_0]\,\Psi^{AD}_{\vec{K}_0}(\vec{R}, \vec{r}_1, \cdots, \vec{r}_n) = 0 \quad . \tag{11}$$

The crucial point here is that the Hamiltonian now only has parametric dependence on the projectile coordinates $\{\vec{r}_i\}$, which appear in the potential, U.

Clearly, for two-body projectiles, the full CDCC approach is more accurate than the adiabatic approach, particularly at low energies. However, the adiabatic model does not suffer so much from convergence issues or computational limitations. Also, it has been generalised and applied to three-body projectiles, something the CDCC method cannot yet cope with. In addition, the adiabatic model allows for certain simplifying insights, such as when only one of the projectile's constituents interact with the target. An example of this is the pure Coulomb breakup of a one-neutron halo nucleus like ^{11}Be, to be discussed later on.

2.4. Glauber methods

A far more efficient approach for dealing with an n-body projectile is to use the few-body Glauber (FBG) model, which is based on the eikonal approximation.

The eikonal approximation was introduced in quantum scattering theory by Moliere and later developed by Glauber who applied it to nuclear scattering where he formulated a many-body, multiple scattering generalisation of the method[18]. In common with other semi-classical approaches, the eikonal method is useful when the wavelength of the incident particle is short compared with the distance over which the potential varies appreciably. This short wavelength condition is expressed in terms of the incident centre of mass wave number, K_0, and the range of the interaction, R_0, such that

$$K_0 R_0 \gg 1 \ . \tag{12}$$

However, unlike short wavelength methods such as the WKB approximation, the eikonal approximation also requires high scattering energies, such that

$$E \gg |V_0| \ , \tag{13}$$

where V_0 is a measure of the strength of the potential. In practice, and when V is complex, this high energy condition is not critical and the eikonal approximation works well even when $E \approx |V_0|$ provided the first condition, equation (12), holds and we restrict ourselves to forward angle scattering.

The eikonal wavefunction has incorrect asymptotics and so, to calculate amplitudes and observables, it must be used within a transition amplitude. Thus for two-body elastic scattering, via a central potential $V(R)$, the transition amplitude is

$$T(\vec{K}_0, \vec{K}) = \langle \vec{K}| \ V \ |\psi^{eik}_{\vec{K}_0}\rangle \ . \tag{14}$$

This leads to the well-known form of the scattering amplitude

$$f_0(\theta) = -iK_0 \int_0^\infty b\, db\, J_0(qb)\, [S_0(b) \ - \ 1\,] \ , \tag{15}$$

where $q = 2K_0 \sin(\theta/2)$, θ is the scattering angle, and $S_0(b) = \exp\left[i\chi(b)\right]$ is the eikonal elastic S-matrix element at impact parameter b, and the eikonal phase shift function, $\chi(b)$, is

$$\chi(b) = -\frac{1}{\hbar v} \int_{-\infty}^{\infty} V(R)\ dz \ . \tag{16}$$

The few-body Glauber (FBG) scattering amplitude, for a collision that takes a composite n-body projectile from an initial state $\phi_0^{(n)}$ to a final state $\phi_\alpha^{(n)}$, can be derived following the same steps as in the two-body (point particle projectile) case. The post form transition amplitude is

$$T(\vec{K}_\alpha) = \langle \phi_\alpha^{(n)}\, e^{i\vec{K}_\alpha \cdot \vec{R}} | U(\{\vec{R}_j\}) | \Psi^{eik}_{\vec{K}_0} \rangle, \tag{17}$$

and we obtain

$$f^{(n)}(\vec{K}_\alpha) = -\frac{iK_0}{2\pi} \int d\vec{b}\, e^{i\vec{q}\cdot\vec{b}}\, \langle \phi_\alpha^{(n)} | S^{(n)}(\vec{b}_1, \cdots, \vec{b}_n) - 1 | \phi_0^{(n)} \rangle, \tag{18}$$

where

$$S^{(n)} = \exp\left[i \sum_{j=1}^{n} \chi_j(b_j) \right] = \prod_{j=1}^{n} S_j(b_j). \tag{19}$$

Thus the total phase shift is the sum of the phase shifts for the scattering of each of the projectile's constituents, as shown in figure (3). This property of phase shift additivity is a direct consequence of the linear dependence of eikonal phases on the interaction potentials V_{jT}.

Corrections to the straight line assumption of the eikonal approximation have been calculated and allow the FBG approach to be applied at much lower energies than expected (below 20 MeV/A). The most straightforward approach is to replace the eikonal S-matrices by the physical ones, while retaining the simplicity of the impact parameter framework of the model [19].

The model generalises in a natural way when Coulomb forces are included in the projectile constituent-target potentials, V_{jT}.

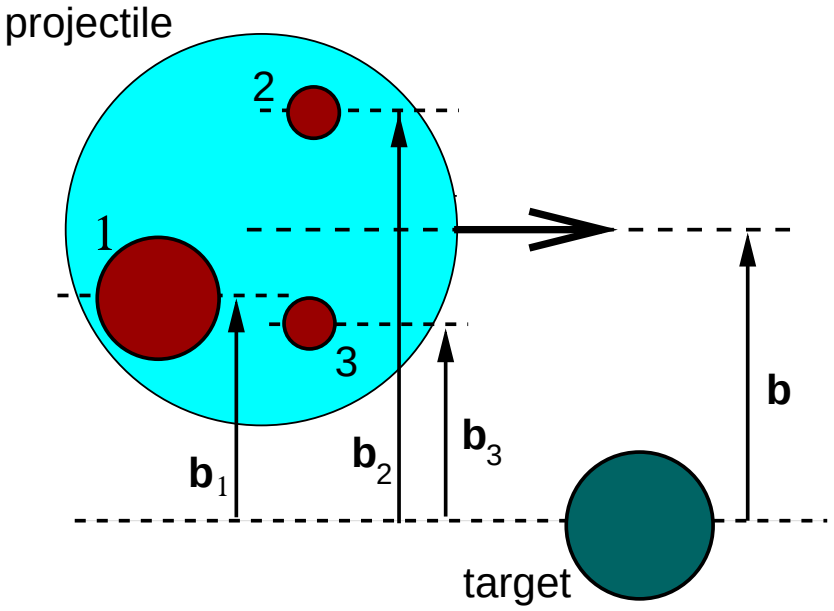


Figure 3. In the few-body Glauber model, each constituent of the projectile scatters from the target independently with its S matrix defined as a function of its own impact parameter.

2.5. The Optical Limit of the Glauber model

The Glauber model can be simplified considerably at high energies when the interaction between each projectile constituent and the target can be considered as purely absorptive. In this case, each constituent S-matrix, $S_j(b_j)$, is calculated within the optical limit of the Glauber model [20]. Here, the eikonal phase shifts are calculated assuming a '$t\rho\rho$' approximation to the optical potentials, V_{jT}, using one-body densities for each j constituent and the target, and an effective nucleon-nucleon amplitude, f_{NN}. The optical limit S-matrices are thus written as

$$S_j^{OL}(b) = exp\left[i\int_{-\infty}^{\infty} dz \int\int d\vec{r}_1\, d\vec{r}_2\, \rho_j(r_1)\rho_T(r_2) f_{NN}(|\vec{R}+\vec{r}_1-\vec{r}_2|)\right]. \quad (20)$$

For an absorptive zero range NN amplitude and an isospin zero target we have

$$f_{NN}(\vec{r}) = (i\bar{\sigma}_{NN}/2)\delta(\vec{r}) \quad (21)$$

where $\bar{\sigma}_{NN}$ is the average of the free nn and np total cross sections at the energy of interest.

It is important to note that we have not thrown away here the few-body correlations in the projectile since at this stage it is only the constituents' scattering via their individual S_j's that has been treated in the optical limit (OL). The few-body S-matrix is still defined according to equation (19). However, if all few-body correlations are also neglected then $S^{(n)}$ is replaced by S^{OL} which is defined as for the individual S_j^{OL} but with ρ_j replaced by the one-body density for the whole projectile. In this case it can easily be shown that full projectile-target OL S-matrix is equivalent to neglecting

breakup effects in equation (18), i.e.,

$$S^{OL}(b) = \exp\left[\langle\phi_0^{(n)}|i\sum_{j=1}^{n}\chi_j(b_j)|\phi_0^{(n)}\rangle\right]. \tag{22}$$

2.6. Cross sections in Glauber theory

The Glauber model provides a convenient framework for calculating integrated cross sections for a variety of processes involving peripheral collisions between composite projectiles and stable targets. In particular, stripping reactions have been studied using approaches developed by Serber[21]. Variants of such methods are still in use today due to the simple geometric properties of the reaction processes at high energies.

In the few-body Glauber model, the differential cross section for the scattering process defined by equation(18) is

$$\left(\frac{d\sigma}{d\Omega}\right)_\alpha = |f^{(n)}(\vec{K}_\alpha)|^2, \tag{23}$$

and the total cross section for populating the final state α is thus

$$\begin{aligned}\sigma_\alpha &= \int d\Omega\ |f^{(n)}(\vec{K}_\alpha)|^2 \\ &= \int d\vec{b}\ |\langle\phi_\alpha^{(n)}|S^{(n)}|\phi_0^{(n)}\rangle - \delta_{\alpha 0}|^2\ .\end{aligned} \tag{24}$$

It should again be noted however that such an expression is only valid at high beam energies and low excitation energies since energy conservation is not respected in this model. When $\alpha = 0$, the total elastic cross section is

$$\sigma_{el} = \int d\vec{b}\ |1 - \langle\phi_0^{(n)}|S^{(n)}|\phi_0^{(n)}\rangle|^2. \tag{25}$$

The total cross section is also obtained from the elastic scattering amplitude, employing the optical theorem, to give

$$\sigma_{tot} = 2\int d\vec{b}\left[1 - \Re\,\langle\phi_0^{(n)}|S^{(n)}|\phi_0^{(n)}\rangle\right]. \tag{26}$$

Hence, the total reaction cross section, defined as the difference between these total and elastic cross sections, is

$$\sigma_R = \int d\vec{b}\left[1 - |\langle\phi_0^{(n)}|S^{(n)}|\phi_0^{(n)}\rangle|^2\right]. \tag{27}$$

For a projectile of total angular momentum j, the above expression is more correctly:

$$\sigma_R = \frac{1}{2j+1}\int d\vec{b}\sum_{m,m'}\left[1 - |\langle\phi_{0m'}^{(n)}|S^{(n)}|\phi_{0m}^{(n)}\rangle|^2\right]. \tag{28}$$

For projectiles with just one bound state, any excitation due to interaction with the target will be into the continuum. For such nuclei, which include the deuteron and many of the neutron halo nuclei (such as ^{6}He and ^{11}Li), it is possible to describe elastic breakup channels in which the target as well as each cluster in the projectile remain in their ground states. For simplicity of notation, we assume a two-body projectile

with continuum wave functions $\phi_{\vec{k}}$, where $\vec{k}$ is the relative momentum between the two clusters, and $S = S^{(2)}(b_1, b_2) = S_1(b_1)S_2(b_2)$ is understood. Elastic breakup, also referred to as diffractive dissociation, has amplitudes

$$f(\vec{k}, \theta) = -iK_0 \int d\vec{b}\, e^{i\vec{q}\cdot\vec{b}} \langle \phi_{\vec{k}\sigma} | S | \phi_{0m} \rangle. \tag{29}$$

Making use of the completeness relation (when there is only one bound state)

$$\int d\vec{k}\ |\phi_{\vec{k}\sigma}\rangle\langle\phi_{\vec{k}\sigma}| = 1 - |\phi_{0m}\rangle\langle\phi_{0m}| \tag{30}$$

the total elastic breakup cross section is

$$\sigma_{bu} = \frac{1}{2j+1} \int d\vec{b} \sum_{m,m'} \left[\langle \phi_{0m}|\ |S|^2 |\phi_{0m}\rangle \delta_{m,m'} - |\langle \phi_{0m'}|S|\phi_{0m}\rangle|^2 \right] . \tag{31}$$

The difference between the reaction and elastic breakup cross section is the absorption cross section,

$$\sigma_{abs} = \frac{1}{2j+1} \int d\vec{b} \sum_{m} \left[1 - \langle \phi_{0m}|\ |S|^2 |\phi_{0m}\rangle \right] , \tag{32}$$

which represents the cross section for excitation of either the target or one or both of the projectile clusters.

The above formula can be understood by examining the physical meaning of $|S|^2$ ($= |S_1|^2|S_2|^2$). The square modulus of each cluster S-matrix element, $|S_i|^2$ represents the probability that it survives intact following its interaction with the target at impact parameter $\vec{b}_i$. That is, at most, it is elastically scattered. At large impact parameters $|S_i|^2 \to 1$ since the constituent passes too far from the target. The quantity $1 - |S_i|^2$ is therefore the probability that cluster i interacts with the target and is absorbed from the system. Such a simple picture is useful when studying stripping reactions in which one or more of the projectile's clusters are removed by the target while the rest of the projectile survives. Thus, the cross section for stripping cluster 1 from the projectile, with cluster 2 surviving, is given by

$$\sigma_{str} = \frac{1}{2j+1} \int d\vec{b} \sum_{m} \langle \phi_{0m}||S_2|^2[1 - |S_1|^2]|\phi_{0m}\rangle. \tag{33}$$

This cross section is seen to vanish if the interaction V_{1T} of constituent 1 with the target is non-absorptive, and hence $|S_1| = 1$.

2.7. Time-dependent methods

A number of other semi-classical few-body reaction models have been developed and applied to reactions in which the projectile is treated as a core+valence nucleon system. One method, developed by Bonaccorso and Brink, is to solve the time-dependent Schrödinger equation after assuming that the relative motion between the projectile's core and the target can be treated classically and approximated by a constant velocity path. This method [22, 23] treats the time dependence of the reaction explicitly and thus conserves energy, but not momentum. Breakup amplitudes can then be calculated

within time dependent perturbation theory, referred to as the Transfer to the Continuum (TC) model [24].

Another time dependent approach, described by Melezhik and Baye [25], also treating the projectile-target relative motion semi-classically, is to solve the time dependent Schrödinger equation using a non-perturbative algorithm on a three-dimensional spatial mesh that allows the treatment of Coulomb breakup in the nonperturbative regime.

3. Reaction cross sections

One of the first observables measured in the study of neutron-rich (halo) nuclei was their total interaction cross section [8, 9]. This was the first indication of their extended matter radii due to the long range tail in their neutron densities. Theoretically, one calculates the total reaction cross section using equation (28). Early estimates of the size of neutron rich isotopes of lithium and helium employed the optical limit of the Glauber model [20] in which the nuclear one-body densities were taken to be simple Gaussians. This allows for a simple analytical expression to be derived [26]. This predicted an enhanced size for these nuclei compared with that obtained from the usual $\langle r^2 \rangle^{1/2} \propto A^{1/3}$ scaling.

By retaining the few-body degrees of freedom in the projectile wave function, its important structure information remains entangled. As a consequence, studies that evaluated the reaction cross section in equation (28) correctly [10, 11], rather than take the optical model limit, predicted an even larger matter radius, as shown in figure (4). This may at first sight seem contrary to what we might expect, since such a model allows for new breakup channels to become available predicting a larger reaction cross section and hence a smaller radius to bring the cross section back down to the experimental value again. However, a simple yet powerful theoretical proof, due to Johnson and Goebel [27], shows that for a given halo wave function, the optical limit model always *overestimates* the total reaction cross section for strongly absorbed particles, thus requiring a smaller halo size than suggested by the full few-body calculation for a given cross section.

4. Elastic and inelastic scattering

Much has been learned about the structure of light exotic nuclei from elastic scattering, whether the nucleus of interest is scattered from a stable nucleus or single proton. The latter case is, of course, just proton elastic scattering in inverse kinematics. Over the past decade, a number of measurements of the angular distribution for the scattering of exotic weakly-bound light nuclei from a stable target (often ^{12}C) were unable to distinguish between elastic and inelastic scattering due to the poor energy resolution in the detectors. Such 'quasielastic' cross sections were thus unable to resolve low-lying excited states of the target (e.g. the 2^+ and 3^- states of ^{12}C) from the elastic channel and the data were an incoherent sum of elastic and inelastic pieces.

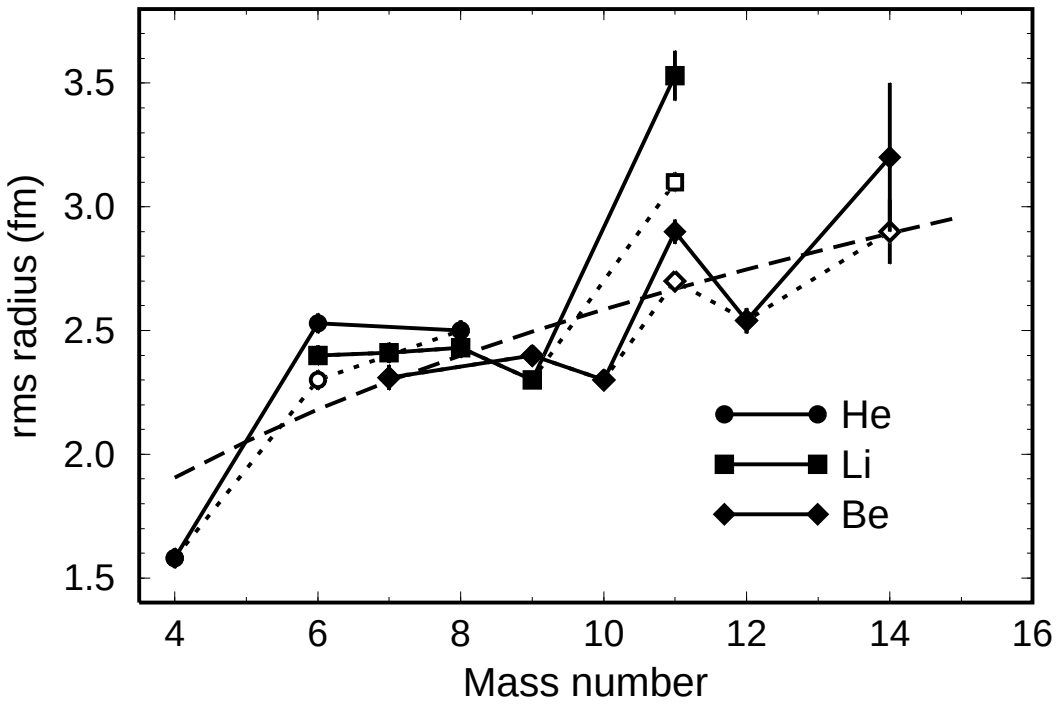


Figure 4. A plot of the matter radii of the isotopes of He, Li and Be as predicted by reaction cross section calculations [10, 11] that are compared with experimentally measured interaction cross sections. The dashed line shows the $R_0 A^{1/3}$ dependance (R_0 = 1.2fm) expected of mean field nuclei. The open symbols, joined by the dotted lines, are the radii predicted using one-body density description of the nuclei within an optical limit approximation. The full symbols are predictions using cluster wavefunctions within a few-body Glauber approach. The open symbols are from the optical limit Glauber model involving one-body densities derived from the same cluster wavefunctions. In both cases, the reaction cross section is fixed to the experimental value.

Angular distributions have been measured for ^{6}He [28], ^{8}He [29], ^{8}B [30], ^{11}Li [31, 32] and ^{14}Be [33]. All these nuclei are very weakly-bound and have a well-defined few-body cluster structure. Indeed, most have only one bound state and any excitation during the scattering process will therefore couple to the breakup channels. Similarities were quickly drawn between these and well-studied examples such as the deuteron (p+n), ^{6}Li (α+d) and ^{7}Li (α+t), the scattering of which is strongly influenced by their dynamic polarization. For such projectiles, simple folding models based on single particle densities fail to generate the optical potentials needed to describe the elastic scattering angular distributions.

For halo nuclei where the binding energies are typically of the order of 1 MeV or less, the breakup effect is even more important. The elastic scattering data for ^{6}He+^{12}C have been analyzed within an optical model approach, with the real part of the optical potential calculated in the double-folding model using a realistic density-dependent

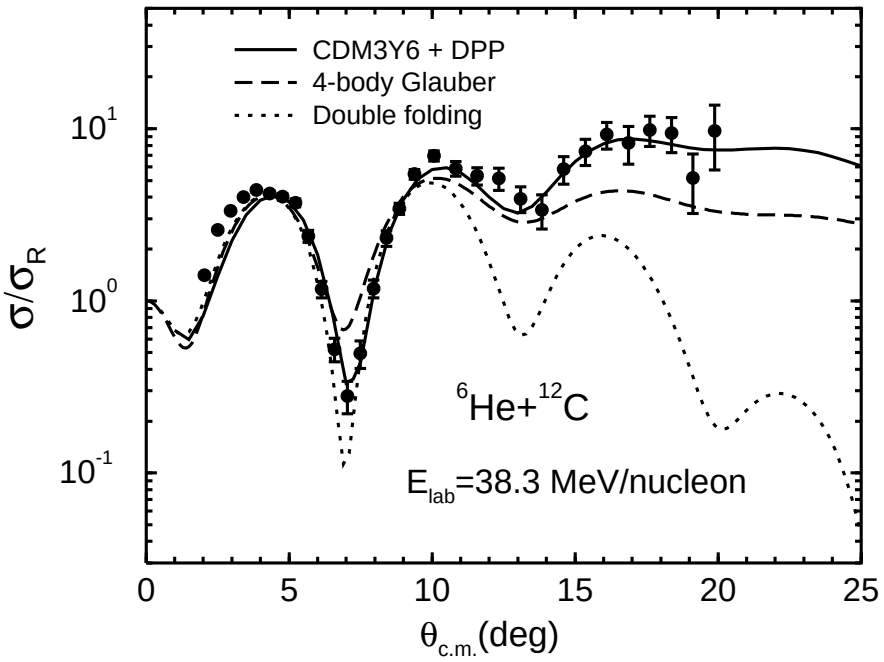


Figure 5. Elastic scattering of ^{6}He+^{12}C at 38.3 MeV/nucleon. The data are from [34]. The solid curve is an optical model fit to the data comprising of a folded potential, using the energy- and density-dependent effective NN interaction CDM3Y6 of [51] folded over simple one-body densities for projectile and target, plus a complex dynamic polarization potential to account for ^{6}He breakup. [See [34] for further details.] The dashed curve is obtained from a completely parameter-free four-body Glauber calculation with a Faddeev wavefunction for ^{6}He [28]. The dotted curve was obtained by folding a ^{6}He density [35] and a 2-parameter Fermi density for ^{12}C with the density-dependent DDM3Y interaction [36].

NN interaction and the imaginary part taken as a standard Woods-Saxon form. The projectile density used in the folding is calculated from realistic few-body wavefunctions. Such a 'bare' folding potential, however, describes the no-breakup scattering in which the projectile remains in its ground state throughout. An additional phenomenological dynamic polarization potential (DPP) must therefore be added to it to account for coupling to the breakup channels [34] (see figure (5)).

A more microscopic approach to elastic scattering is to use a few-body scattering model in which the few-body correlations of the projectile are retained. In such an approach it is the few-body wavefunction of the projectile that is used directly rather than its one-body density. Three-body models used previously to study the scattering of deuterons and ^{6,7}Li have been based on CDCC, adiabatic and Glauber approaches. The required inputs to all these models, in addition to the projectile few-body wavefunction, are the projectile constituent-target optical potentials. In this way, breakup effects are included in a natural way. In particular, one of the advantages of the Glauber approach

is that breakup is included in a natural way to all energies and angular momenta, and to all orders in breakup, through a closure relation. In fact, it has been found that higher order breakup terms, such as those responsible for continuum-continuum coupling, are indeed very important [37].

The DPP representation of this breakup effect on the elastic channel has been analyzed for various halo nuclei such as ^{6}He and ^{11}Li [34, 37, 38, 39, 40]. It is found to be strongly absorptive and with a significant repulsive real part in the far surface region, which acts to reduce the far-side scattering amplitude.

Most few-body models have been developed to describe the scattering of two-body projectiles (three-body scattering models). However, many have been extended to four-body models in order to describe the scattering of projectiles which are themselves modeled as three-body systems, such as ^{11}Li. First, a four-body Glauber model, based on eikonal and adiabatic methods, was presented [41] and subsequently extended to include recoil and few-body correlation effects [42]. Soon after, a four-body adiabatic model - which was fully quantum mechanical in that it made no semi-classical or eikonal assumptions - was developed [43] based on the three-body model of Johnson and Soper [17]. At the time of writing this review, work is underway on a four-body CDCC calculation. Ultimately however, the simplicity of the Glauber approach makes it the most practical tool for describing the scattering of projectiles composed of more than three constituents. Using random sampling (Monte Carlo) integration, it has been extended [44] to describe the scattering of ^{8}He from ^{12}C in which the projectile is described by a five body (α+4n) harmonic oscillator based Cluster Orbital Shell Model Approximation (COSMA) wavefunction [45].

An analysis of high energy (700 MeV) elastic scattering of protons from helium isotopes, ^{6}He and ^{8}He, in inverse kinematics has been carried out [47, 46] to estimate their matter radii (figure (6)). Using the Glauber model to determine the forward angle differential cross section it was found that while few-body correlation effects were not important at the small momentum transfers of the experimental data [48], nevertheless the asymptotic behaviour of the few-body wavefunctions describing the ground states of these nuclei lead to long-range tails in the one-body density distributions, particularly for ^{6}He. Simple analytical expressions for the densities do not give rise to such long tails and hence under-predict the matter radius of ^{6}He by about 10%.

An important drawback of Glauber methods is that they are only accurate for forward angle, high energy, scattering. At lower energies, corrections to the two basic assumptions (the eikonal and the adiabatic) of the few-body Glauber model are necessary [19, 49]. Figure (7) shows the ratio to the rutherford angular distribution for ^{11}Be elastic scattering from carbon at 10 MeV/nucleon, using various models. The solid curve is the CDCC cross section and represents here an 'exact' calculation; the dot-dashed is also from a fully quantum mechanical calculation but having made an adiabatic approximation; while the dashed curve is from a three-body Glauber model calculation which makes, in addition to adiabatic assumption, an additional semi-classical (eikonal) approximation. Clearly, while this energy is rather low for either the eikonal or adiabatic

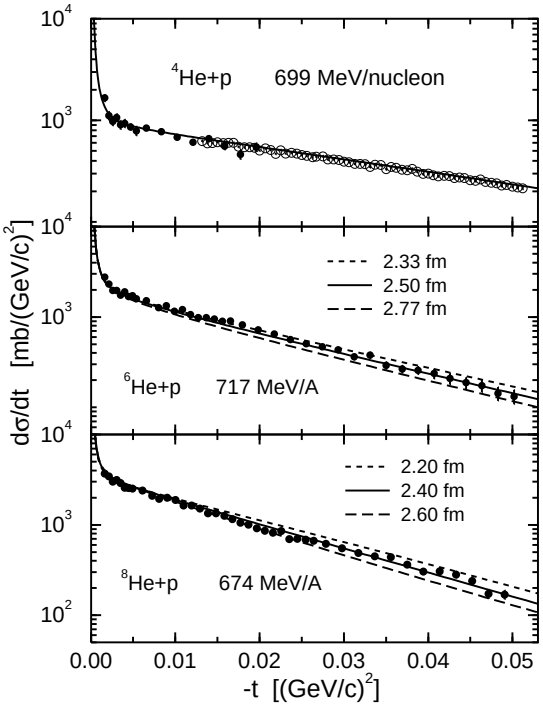


Figure 6. Elastic scattering of ^{4,6,8}He from protons at intermediate energies. At small momentum transfers such as these the cross sections depend on the matter radii chosen for the projectiles. The curves for ^{6}He and ^{8}He scattering were obtained within a few-body Glauber model [47]. The data are from The IKAR collaboration [48, 46].

assumptions to hold, both can be corrected for [19, 49] with the inclusion of non-eikonal and non-adiabatic terms in the elastic amplitude.

A useful approximation to the adiabatic model, referred to as the 'recoil limit' model [13, 50], is obtained when the potential between the projectile's core and the target dominates over that between the valence nucleon(s) and the target. In this limit, when all but one of the potentials in the sum in equation (2) can be neglected, it can be shown that there is an exact closed form to the few-body adiabatic wavefunction of equation (11). This leads to a factorised expression for the scattering amplitude, into a point amplitude that is, to a good approximation, that of the core-target system at the same energy per nucleon and momentum transfer as the full projectile, and a form factor containing all the information on the structure and excitations of the projectile. Such a simple formulation has proved to be extremely useful not only in providing physical insight but as a check of more complete coupled channels methods such as the adiabatic and CDCC models.

The advantage of the few-body scattering models described here is that they require two types of inputs which should, in principle, be well-known: (i) the few-body wavefunctions that describe the structure of many of the loosely-bound, particularly

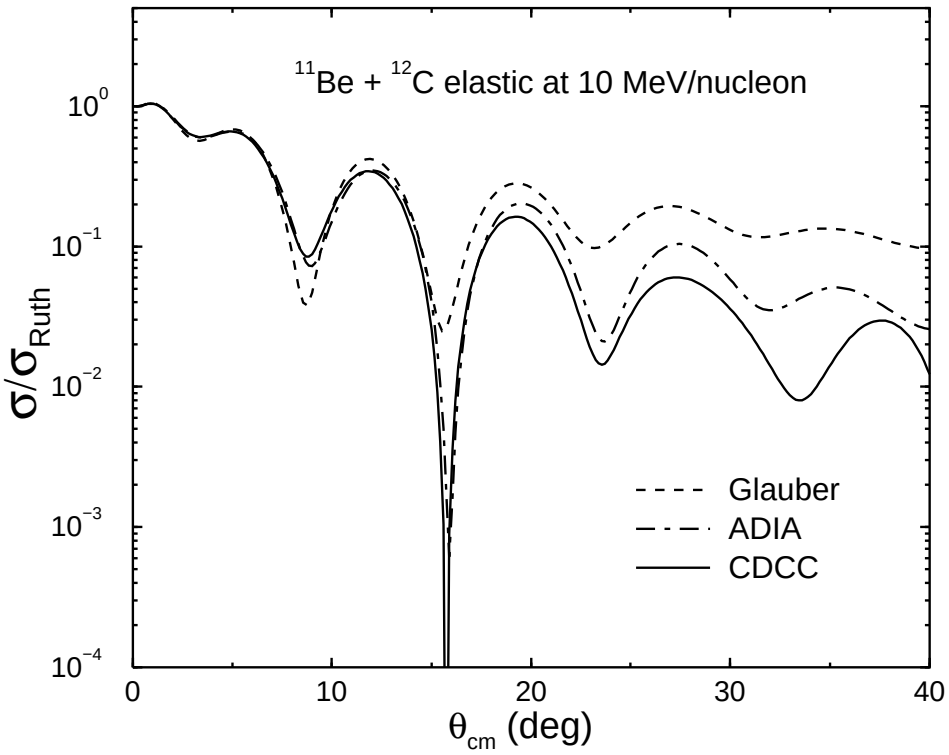


Figure 7. Calculated differential cross sections for the elastic scattering of ^{11}Be from ^{12}C at 10 MeV/nucleon using various three-body models: Glauber (dashed curve), adiabatic (dot-dashed curve) and CDCC (solid curve) [19, 49]. The importance of both non-adiabatic and non-eikonal corrections at larger scattering angles can be seen clearly at these relatively low scattering energies. No data exist.

light halo nuclei so well and (ii) information about the individual scattering of the projectile clusters from the target, either as optical potentials or as scattering amplitudes. It is now well-established that the few-body dynamics should be incorporated into the scattering and reaction mechanisms *ab initio*. This necessary entangled approach goes beyond simply feeding in knowledge of the total matter density distribution of the projectile.

Another approach that takes into account the few-body nature of scattering of halo nuclei is to treat it within a few-body multiple scattering approach. Such a model, known as the Multiple Scattering expansion of the total Transition amplitude (or MST), has been developed by Crespo [52]. While traditional multiple scattering expansions of the optical potential, such as the KMT approach [53], rely on a mean field description that treats all nucleons (in the projectile and target) on an equal footing, they are inappropriate for exotic loosely-bound nuclei that are far from stability. The MST approach, however, surpasses such mean field expansions since it takes into account structure features of the projectiles beyond the total matter density distribution alone. It has been applied to proton elastic scattering from ^{11}Li, in inverse kinematics, and shows a much better agreement with data than the KMT optical model approach due

to its inclusion of both recoil effects (of the ^{9}Li core) and breakup effects of the halo neutrons [54].

Proton inelastic scattering from halo nuclei has been used as a tool to search for evidence of the low-lying excited states in the continuum. So far, coupled channels methods such as CDCC, which explicitly expand on continuum states, can only be used, as mentioned earlier, to study projectiles comprising two clusters. But many exotic nuclei present a core + 2n three-body structure and thus require for the time being a different approach. The reaction $^{11}\mathrm{Li}(p,p')^{11}\mathrm{Li}^{*}$ has been analysed within both the shake-off approximation [55], in which only the proton-core contribution to the single scattering term is considered, and the multiple scattering MST approach [56], in which the scattering of the proton from the halo neutrons is also taken into account.

A microscopic model, referred to as the g folding potential has been developed by Dortmans and Amos [57] who, together with Karataglidis [58], applied it to both elastic and inelastic proton scattering on a range of both stable and unstable nuclei. The optical potential for the model is obtained by folding a complex energy- and density-dependent effective NN interaction over the one-body density matrix elements and single particle bound states of the target generated by shell model calculations. They show that the analysis of inelastic data is a sensitive test of nuclear structure. For instance, it has been shown [59] that good agreement with data can be achieved for the inelastic scattering to the unbound 2^{+} state at 1.87 MeV of ^{6}He from protons at 41 MeV/A, provided a large enough shell basis is used to calculate the wavefunctions for the initial and final states of ^{6}He.

5. Breakup reactions

Given their very low binding energy, breakup cross sections of exotic nuclei are generally quite large and relatively easy to measure. Consequently, numerous breakup measurements have been performed, even when the radioactive beam intensity was rather low. In parallel, the theoretical community has been attempting to model these reactions accurately. In the following sections we discuss the results for several approaches available in the literature.

5.1. Time-dependent calculations (Semi-classical and Glauber approaches)

The semiclassical theory for Coulomb excitation was developed in the early days of nuclear physics [60]. The semiclassical approach is valid for large impact parameters and relies on the fact that the relative motion between the projectile and target can be treated classically whilst the excitation of the projectile is treated quantum mechanically. Then, the total breakup cross section is a product of the Rutherford cross section by the square of the excitation amplitude. The excitation amplitude is typically calculated perturbatively, and often only E1, M1 and E2 contributions are sufficient. A further extension of this work for relativistic energies, where the projectile follows straight line

trajectories, can be found in [61].

The pioneering work by Baur and Bertulani [62], proposing Coulomb dissociation as a source of information for radioactive capture rates relevant in astrophysics, justifies the large efforts that concentrated on this topic over the past decade and in particular on the breakup of ^{8}B. (For more detail, a topical review on this subject can be found in [63]). Calculations in [62] show the kinematical regimes where the breakup of ^{7}Be$\rightarrow \alpha+^{3}$He and ^{16}O$\rightarrow \alpha+^{12}$C on ^{208}Pb would become useful for astrophysics (both reactions rates have meanwhile been measured using the Coulomb dissociation method). More relevant for our topic is the application to ^{8}B. In [64], calculations for the E1 and E1+E2+M1 are performed and compared with the RIKEN data [65]. Controversy on the importance of the E2 contribution for this reaction was raised due to the re-analysis of the data in [66]. Improvements to the reactions models, which will be covered in the following subsections, have shown that the quadrupole contribution is not easy to disentangle.

Higher order corrections to include the two photon exchange was developed in [67] and corrections up to third order for the Coulomb interaction was deduced within the small adiabaticity approximation [68]. The second order correction is always positive but the third order interferes to produce the so called dynamical quenching of the E2 strength [69]. These corrections are more important at lower beam energies and for small relative energies of the fragments resulting from the breakup of the projectile. In addition, nuclear diffraction effects need also be considered. The semiclassical approach neglects the strong interaction between the projectile and the target. Diffraction corrections on the Rutherford orbit were calculated by comparing the semiclassical expressions with the Glauber approach [68]. These effects can become very large even for small angles.

Although the first order semiclassical method is appealing due to its simplicity, there are many aspects of the problem that are left out. One of the debated issues concerned the post-acceleration of the light fragment in the Coulomb field. In order to describe this process properly, one should formulate the problem non-perturbatively.

Instead of treating the time dependent Hamiltonian perturbatively, an exact treatment can be performed. This approach, known as the dynamical method and introduced in section 2.7, has two great advantages: i) it contains the coupling to breakup channels to all orders and ii) the multipole expansion of the Coulomb interaction is not necessary. In most applications to data, the projectile is still confined to the Rutherford trajectory. Such applications include the breakup of ^{11}Li (using a dineutron model) and ^{11}Be [70, 71]. The time evolution of the projectile wave function was calculated by solving the three-dimensional time dependent Schrödinger equation. In both examples the dynamical calculation reduces the cross section when compared with first order perturbation theory, although this effect is more noticeable at lower energies. An example of the breakup of ^{11}Li on ^{208}Pb at 28 MeV/A is shown in figure (8), comparing the first order perturbation theory with the time dependent dynamical calculation. The re-acceleration is produced automatically in the calculation, shifting the momentum distributions. The comparison with the breakup data for ^{11}Be is good. For ^{11}Li, the calculation produces a different energy distribution, a limitation not of the

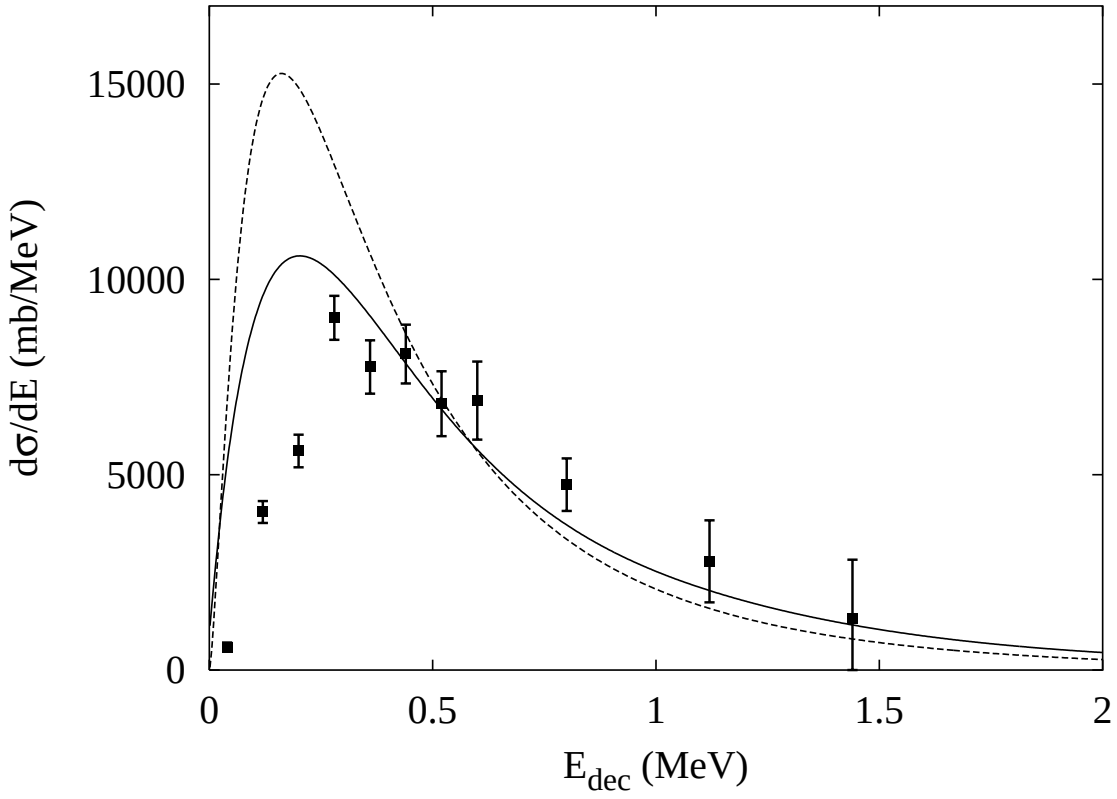


Figure 8. The breakup of ^{11}Li on a lead target at 28 MeV/A: first order perturbation theory (dotted line) versus the dynamical calculation (solid line). The calculations are from [70] and the data is from D. Sackett *et al.*, Phys. Rec. C 48 (1993) 118.

reaction model but of the dineutron structure model. The application of this method to the breakup of ^{8}B at intermediate energies [64, 69] shows the importance of including all the dynamics, as in this case there is a strong E1/E2 interference that reduces substantially the breakup probability.

More recent time-dependent calculations including both the nuclear and the Coulomb interaction between projectile and target have been performed for the low energy breakup of ^{8}B [72, 73]. In the first of these, the calculation is partly truncated, in the sense that no continuum-continuum couplings are included. The comparison between these two calculations shows that this is not an adequate approximation for this system. Similar calculations were performed for the breakup of ^{17}F, another exotic nucleus on the proton dripline [74]. Conclusions are qualitatively similar to those for ^{8}B.

Other implementations of the non-perturbative time dependent approach were performed by [25] and [75]. The Lagrange-mesh method of [25] used the breakup of ^{11}Be on ^{208}Pb at 72 MeV/A as a test case. A careful study of the convergence of the method demonstrates that the equation needs to be solved for a radial grid within a large range ($R_{max} = 1200$ fm) keeping the radial step very small. Deflection from the

straight line trajectories and a spin-orbit coupling to the Coulomb field are included but proven to be weak for the particular case studied. The calculations in [75] have been successful in analysing the recent ^{11}Be data from GANIL.

Another possibility for calculating neutron breakup observables for nuclei on the neutron dripline is the semiclassical TC (Transfer to the Continuum) model [24] described in subsection 2.7. In this model, the initial and final wavefunctions are approximated to their asymptotic forms, and the WKB approximation is made to the distorted waves describing the projectile-target relative motion, providing a simple analytic expression for the Coulomb breakup amplitude. It is generally applicable to reactions at large impact parameters and intermediate energies. It has been demonstrated that this model reduces to the PWBA (Plane Wave Born Approximation) when the binding energy of the projectile tends to zero, and to the Serber formula in the high energy limit.

Often, an independent treatment of the nuclear and Coulomb parts is preferred. For example, in [76] a semiclassical model is developed to study interference effects in the breakup of one-neutron halos. Results for ^{11}Be are calculated when it reacts with three separate targets. The Coulomb breakup contribution is calculated within a first order semiclassical approach, whereas the nuclear neutron-target interaction is treated to all orders. These are finally added incoherently. More recently, the same authors have presented a model in which they calculate both Coulomb and nuclear breakup to all orders consistently within an eikonal framework [77].

Unfortunately, even though it is now generally known that dynamical effects are very important, often the first order semiclassical theory is still used (e.g. the dissociation of ^{19}C [78] or ^{8}He [79]).

5.2. DWBA calculations

A traditional quantum mechanical approach to the breakup reaction uses distorted waves for the initial and final states of the relative motion between the projectile and the target, as well as the Born approximation: the one-step DWBA. The nuclear part of early RIKEN data for ^{8}B breakup on ^{208}Pb was analyzed using this approach [65], whilst the Coulomb part was treated in first-order semiclassical theory. This reaction was re-measured with better accuracy and angular coverage [80]. These data were re-analyzed using DWBA for both nuclear and Coulomb [81, 82]. The results show evidence for the strong model-dependence of the E2 contribution.

At lower energy, the E2 component becomes stronger. A series of experiments were carried out in Notre Dame [83, 84, 85] with the aim of pinning down this ingredient. The DWBA calculation of [86] for this system used, instead of the conventional collective model for the coupling, the folding with the ^{8}B wavefunction. This aspect is essential for loosely bound projectiles. A calculation for the angular distribution, for Coulomb only, shows that the finite range effects of ^{8}B become noticeable for angles as low as 30 degrees, much lower than what would be expected through impact parameter considerations.

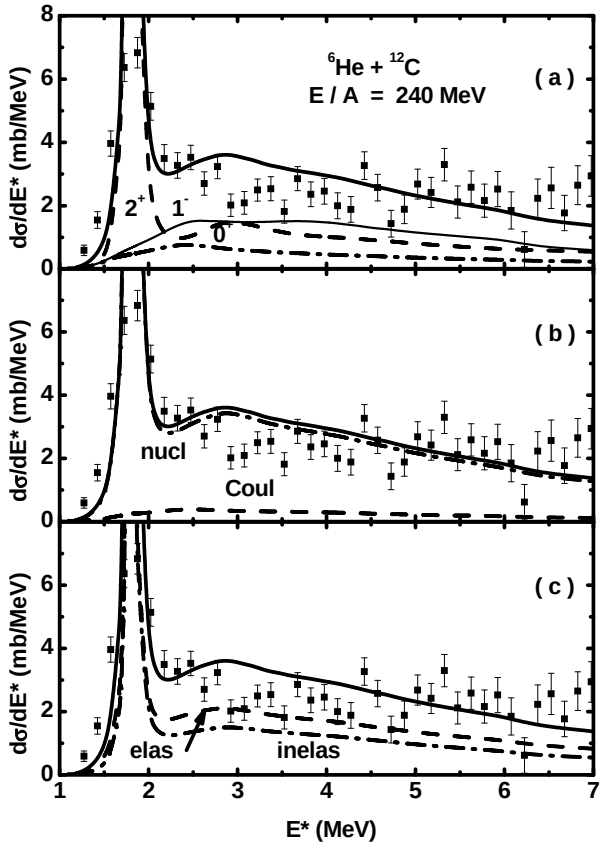


Figure 9. The breakup of ^{6}He on ^{12}C at 240 MeV/A: a) contribution of 1^- (thin solid), 2^+ (long dashed) and 0^+ (dot-dashed) to the differential cross section; b) contribution of the nuclear (dot-dashed) and the Coulomb part (long dashed); c) contribution of elastic (long dashed) and inelastic fragmentation (inelastic). In all cases the thick solid lines correspond to the total differential cross section and are compared with the data from T. Aumann *et al.*, Phys. Rev. C 59 (1999) 1252.

In that work a nuclear peak is predicted around 80 degrees, which disappeared once all couplings were included (next subsection). The importance of Coulomb-nuclear interference is also underlined.

All the above mentioned approaches describe the breakup of two body projectiles. The work for calculating the three body breakup cross section was initiated with the development of the four-body DWIA (Distorted Wave Impulse Approximation) [87]. This method offers a one step quantum mechanical calculation only valid for high energies, when the loss of energy in the breakup is small compared with the initial energy. The calculations were applied to ^{6}He breakup in the fields of ^{12}C and ^{208}Pb. Results show that including the full three body structure of the projectile enables a very rich interplay between the reaction mechanism and the halo excitations that otherwise would be missing (an illustration is given in figure 9). The major drawback of this model is that the four body partial wave expansion is extremely cumbersome. Preliminary four-body DWBA calculations for the Coulomb breakup of ^{6}He have also been presented in

[88].

5.3. CDCC calculations

The CDCC method [89, 90] briefly introduced in section 2.2, offers one of the most complete approximation to the three body problem involving a 2-body projectile impinging on a target. It has been shown that the exact Faddeev equations reduce to the CDCC equations as long as the model space is sufficiently large [91]. And even though convergence issues need to be carefully checked, solving the CDCC equations is much easier than finding the Faddeev solutions to the problem.

The CDCC method reduces to the DWBA when only one-step processes are taken into account. One can further solve the coupled channel equations iteratively, including 2,3,...,n steps in the reaction. This method should obviously converge to the CDCC exact solution.

Before discussing specific applications of the CDCC method, we emphasize that it is not always trivial to obtain a model space which is sufficient to account for all the physical properties (e.g. [16]). Convergence studies concerning the choice of the discretization were performed in Ref.[92] for ^{58}Ni elastic and breakup reactions, proving that both the average method and the midpoint method provide the same results. However, it should be stressed that that study considered nuclear coupling only, and not Coulomb. The main advantage of the average method is that the resulting bin-wavefunctions characterizing the continuum states are square integrable and thus couplings between two continuum states are tractable.

The first application of the CDCC method to the breakup of exotic nuclei was performed for the Notre Dame experiments [83, 84, 85]: 25.8 MeV ^{8}B, breaking into ^{7}Be+p under the field of ^{58}Ni [16, 93]. In [93] differential cross sections for multi-step processes are calculated for both nuclear and Coulomb separately. It is shown that even six-step processes have a significant contribution. Here too, Coulomb and nuclear effects need to be included coherently, as interference plays an important role. In figure (10) the full CDCC calculation is compared with the truncated calculation where no continuum-continuum couplings are included. The huge reduction of the nuclear peak can be only attributed to the couplings within the continuum. The three-body observables were adequately derived in [16]. This piece was required due to the fact that the data had incomplete kinematics [83, 84, 85] (the outgoing proton was not detected). The calculated ^{7}Be angular and energy distributions could then be compared directly with the data. The agreement is excellent for all but the largest detection angle, where transfer effects become relevant. Yet even this fact can be easily accounted for within the model [85].

More recently there has been an application of the CDCC method to the breakup of ^{8}B at higher energies [94]. In the previous years, a series of ^{8}B Coulomb dissociation experiments were performed at MSU [95, 96, 97]. Breakup data on both Pb and Ag targets, at 44 MeV/u and 81 MeV/u, were compared with CDCC calculations in [94].

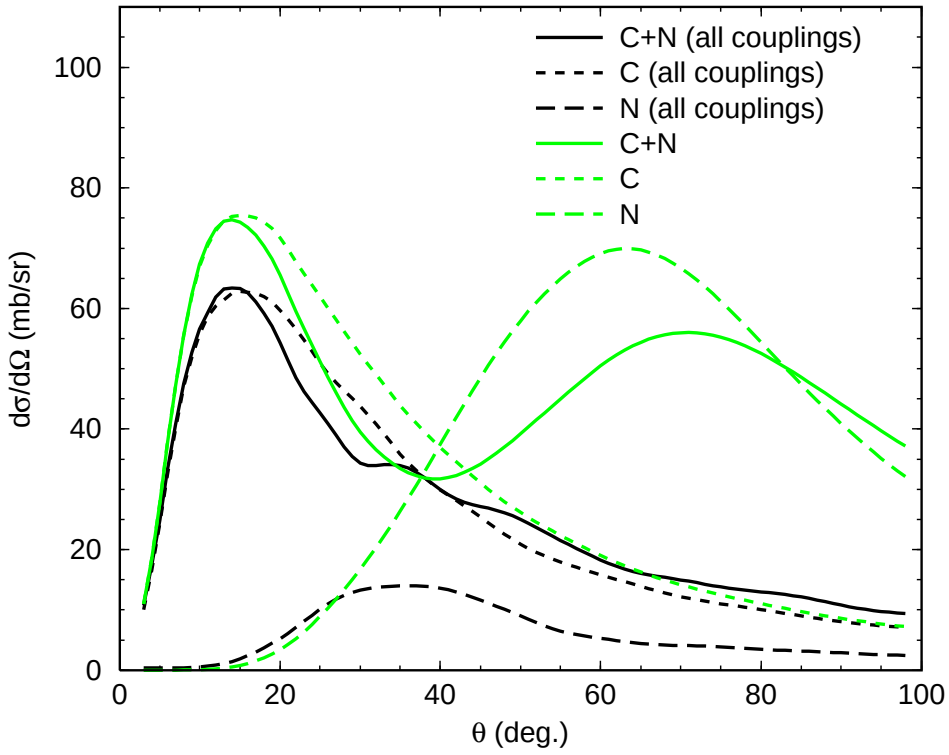


Figure 10. The breakup of ^{8}B on ^{58}Ni at 26 MeV: nuclear only (dashed line), Coulomb only (dashed) and the result of including both nuclear and Coulomb (solid). The grey lines are the truncated calculations without couplings between continuum states.

Therein it is shown that the asymmetry of the momentum distributions is reduced through the couplings to the continuum, in agreement with the results at lower energy [16]. Also, in order to obtain agreement with the data, it was found that the quadrupole component needed to be scaled by 1.6, as shown in figure (11).

The motivation for both the Notre Dame and the MSU series of measurements on ^{8}B is astrophysical. As mentioned earlier, Coulomb dissociation may offer a powerful tool for extracting S-factors, as long as the E2 component can be well determined, nuclear effects are negligible and no higher order effects are present. Both Notre Dame and MSU experiments aimed at pinning down the E2 components, that are part of the dissociation cross section but do not contribute to the direct capture transition at low energy. The data from Notre Dame [85] is consistent with the modified ^{8}B model from Esbensen and Bertsch [69] (where all breakup states are calculated with the ground state single particle interaction). However, as just mentioned, the MSU data [97] requires a 1.6 increase of the E2 component. It is not clear whether the inconsistency comes from the reaction model or missing structure information.

CDCC calculations for the breakup of ^{6}Li and ^{7}Li on Pb have been used to analyze the recent data from Florida State [98]. Experiment shows that the α-breakup for ^{6}Li is systematically larger than for ^{7}Li. The CDCC results predict the correct trend

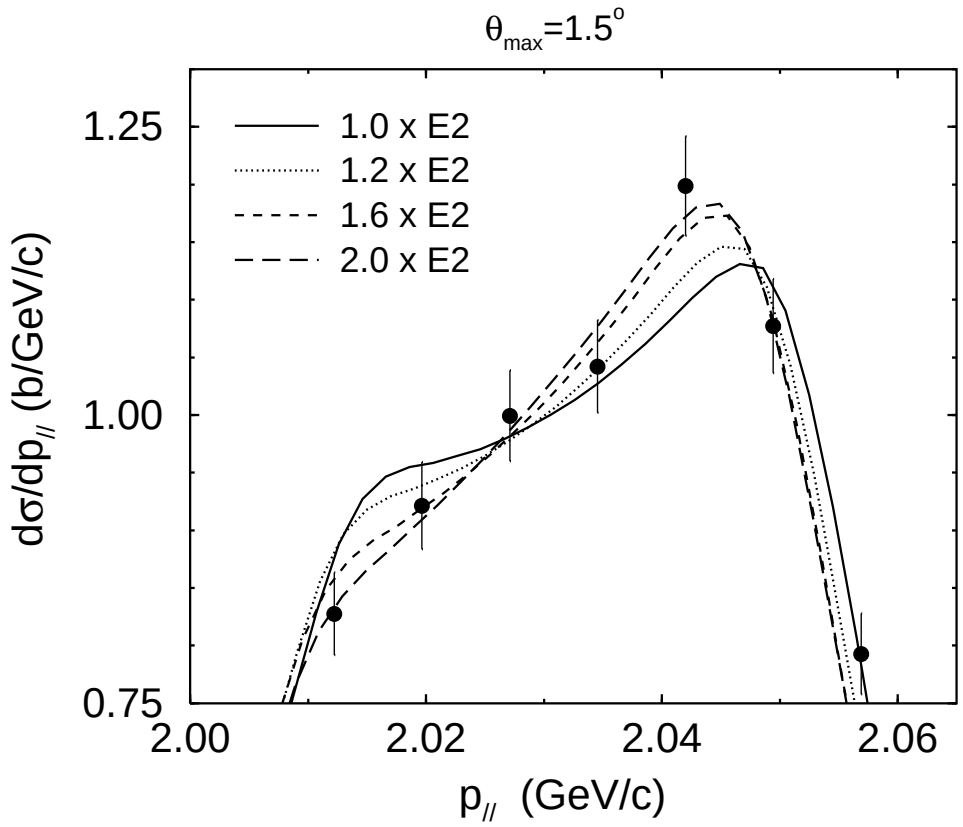


Figure 11. The breakup of ^{8}B on lead at 44 MeV/A: the quadrupole components of the reaction process has been multiplied by the given factor. The data is from [97].

in the measured energy range (29 MeV to 52 MeV) although the absolute value is considerably lower than expected. The most likely reason pointed out by the authors for this mismatch [98] is the absence of transfer channels in the calculation. This was also found to be important for ^{6}He [99] and we will come back to this point in section (7).

5.4. Other approaches to Breakup

Although in the previous subsections we have covered the main theoretical approaches to breakup, some alternative methods, that were developed with specific applications in mind, should also be mentioned.

The adiabatic method described in Subsection 2.3 is particularly interesting for neutron rich nuclei [100, 101]. This method involves a fully quantum-mechanical non-perturbative description of the pure Coulomb breakup process, where essentially two approximations are made: i) the valence particle(s) of the projectile does(do) not interact with the target and ii) the relative motion of the fragments in the projectile is treated adiabatically. This method is thus only applicable to projectiles with a neutral valence particle (such as ^{11}Be) and for reactions performed at relatively high energy. In [100]

results for the breakup of the deuteron are compared with various sets of data, and a good level of agreement is obtained. The application to three body projectiles is made in [101]. The comparison of the theory with the experimental data for the breakup of ^{6}He shows that for this reaction [102], nuclear effects are considerable and finite range effects on the Coulomb interaction need to be taken into account.

Even though the equivalence between the full Faddeev formalism and the CDCC truncation has been proven [91], in practice the CDCC calculations are truncated in configuration space and matched to two body asymptotics. Work developed by Alt and Mukhamedzhanov [103] estimated the correction to these approximations, handling the Faddeev two- to three-body scattering problem. The improvement is that the asymptotics for the three charged particles final state is correctly included. The application to the breakup of ^{8}B shows that these asymptotic effects are more important for larger angles/larger relative energies. They are not relevant for the high energy GSI experiment [104] but should not be neglected in the RIKEN data [65, 80].

The participant spectator model (PSM) has been proposed to calculate high energy reaction observables for three body projectiles impinging on a target. It takes the sudden approximation (neglecting completely the internal energy of the projectile) and assumes that only one of the constituents of the three body nucleus interacts with the target at a time. Initially applied to light targets, where the process was nuclear dominated [105, 106], it has meanwhile been extended to treat Coulomb processes too [107]. A wide variety of observables are computed. For the ^{11}Li data, it seems to be possible to choose reasonable radial cutoff parameters within a black disk approximation, for each fragment separately, that provide an overall agreement.

In the data analysis of many three body breakup experiments, the mechanism is often interpreted as a decay through the existing two-body resonances of the subsystems. In [108] it is shown that a correspondence between the R-matrix resonance parameters and the real resonance structure of the two body subsystems is not always possible.

5.5. Momentum distributions

Measurement of the momentum distributions of the fragments (core and valence nucleons) following the breakup of halo nuclei on stable targets is now a well-established method for studying halo properties. While it has been used for many decades as a tool to access the structure of stable nuclei, it is particularly well-suited to loosely bound systems. The basic idea is simple: since very little momentum transfer is required in the breakup process to dissociate the projectile fragments, they will be detected with almost the same velocity as they had prior to breakup, and their relative velocities will be very similar to those within the initial bound projectile. In all reactions with weakly-bound systems the momentum distributions are found to be very narrowly focussed about the beam velocity. This has the simple physical interpretation of representing the momentum distribution of the initial projectile. Via the Uncertainty Principle, the narrow momentum distribution corresponds to a wide spatial distribution. It was such

observed narrow distributions which first helped confirm the large extent of halo nuclei [109]. Since then, many measurements have been made, involving detection of both the valence nucleons and the core fragments, and the halo structure of several light nuclei has been established.

Two types of distributions can be measured: either perpendicular (transverse) or parallel (longitudinal) to the beam direction. It is now known that the transverse distributions are broadened due to nuclear and Coulomb diffraction effects (elastic scattering of the fragments from the target) and therefore require more careful theoretical analyses. This is why longitudinal momentum distributions are regarded as a better probe of the projectile structure. Early on, simple models, based on eikonal assumptions agreed with measurements rather well. Similar widths were obtained from nuclear breakup on light targets and Coulomb breakup on heavy targets, supporting the view that the distributions were no more than the square of the Fourier Transform of the projectile ground state wavefunction. However, presently this view is considered too simplistic. Firstly, these simple models only really sample the momentum content of the single particle wavefunction at the nuclear surface [111]. Secondly, reaction mechanisms, for the case of two neutron halo nuclei, need to be taken into account since the neutrons may be scattered or absorbed separately. Even for single valence nucleon systems, such as ^{8}B, the reaction mechanisms lead to a narrowing of the calculated width due to the valence proton being in a relative p-state and the $m = \pm 1$ components of the wavefunction being affected differently in the breakup process [69, 112].

For single valence nucleon systems, the longitudinal inelastic breakup momentum distributions for the core - at high energies the elastic breakup piece is small - can be expressed as

$$\frac{\mathrm{d}\sigma}{\mathrm{d}k_z} = \frac{1}{2l+1}\sum_{m=-l}^{l}\int d\vec{s}\,\left|\frac{1}{\sqrt{2\pi}}\int dz\, e^{ik_z z}\,\phi_{lm}(\vec{s},z)\right|^2 \times \int d\vec{b_c}\,|S_c(b_c)|^2\left(1-|S_n(b_n)|^2\right), \qquad (34)$$

where $b_n = |\vec{b_c} + \vec{s}|$ and $\vec{s}$ is the projection of the core-nucleon relative coordinate onto the impact parameter plane, $\phi_{lm}(\vec{s},z)$ is the valence nucleon wavefunction with orbital angular momentum lm and S_c, S_n are the core and nucleon elastic S-matrices as described in Subsection 2.4. The integral over $\vec{b}$ in Eq. (34) represents the reaction mechanism and involves the product of the core survival probability (in its ground state) and the nucleon absorption probability by the target. Without this factor, the momentum distribution is just a Fourier transform of the nucleon wavefunction.

Figure (12) shows a segment of the segre chart with the momentum distributions for individual nuclides superposed. The theoretical curves were obtained using a Glauber model with JLM parameterisation of the optical potentials and incorporating second order non-eikonal corrections (see ref. [110] for details).

Another complication is the possibility of final state interactions between the surviving fragments. These can lead to 2- or 3-body resonances that also act to make the widths narrower [108, 113, 114, 115, 93].

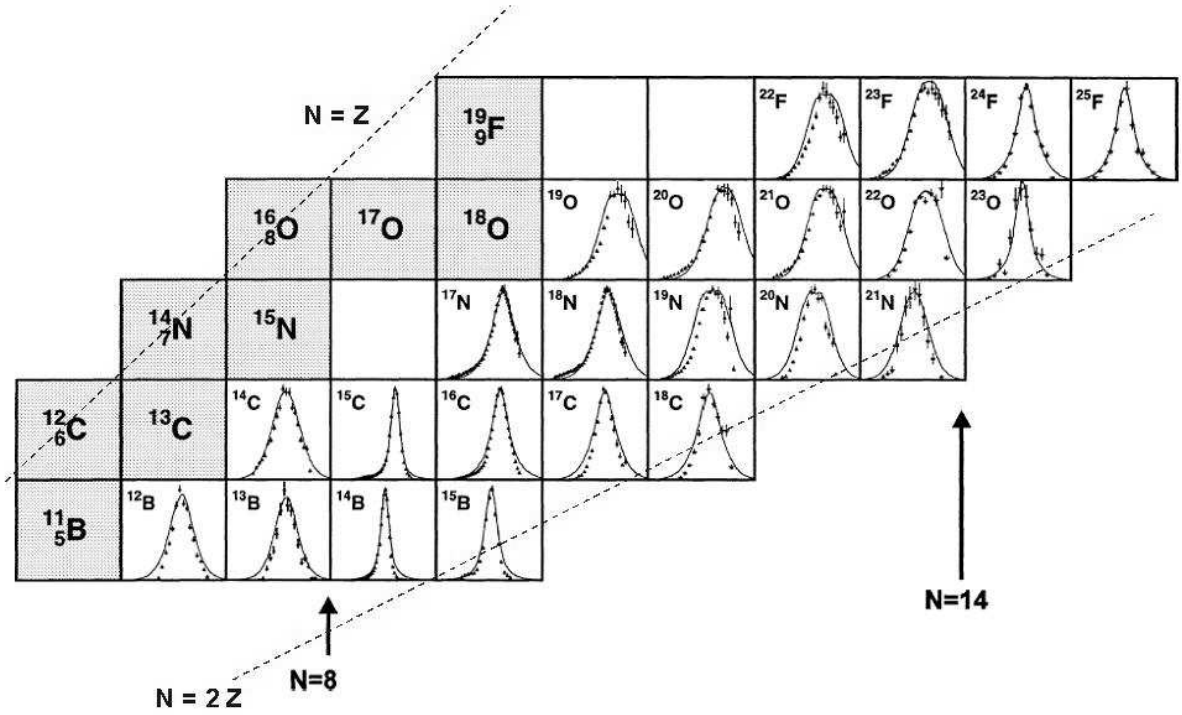


Figure 12. The longitudinal momentum distributions for the core fragments following single neutron removal from a range of neutron-rich nuclides on a carbon target [110]. The narrow distributions correspond to larger size.

Finally, in measurements in which the surviving fragments formed a bound state, there was a significant probability that the reaction would populate excited states of this system. This implied that the measured momentum distributions contained several distributions superimposed, each with a different width. This has led to gamma-ray coincidence measurements to discriminate between the different partial cross sections, as will be discussed in the next section.

6. Knockout reactions

The early measurements of Coulomb dissociation and one nucleon removal cross sections of halo states have since evolved into the more general technique of single neutron knockout reactions, which have become a reliable tool for obtaining basic information about the shell structure of a number of neutron-rich nuclei. The neutron knockout process takes place via two different mechanisms: diffractive dissociation (elastic breakup) and stripping (neutron absorption by the target). Theoretically, each of these two contributions is evaluated separately, usually within a Glauber framework. In particular,

the stripping cross section can be calculated within a model in which the projectile comprises of the stopped neutron plus the surviving fragment. Such a 'three-body' model (fragment+neutron+target) treats the detected fragment as a 'spectator core' which, at most, interacts elastically with the target.

The spectator core assumption in models of nuclear-induced breakup or a knockout reaction was first proposed by Hussein and McVoy[116] and has more recently been applied to the study of the break-up of halo nuclei[117, 118] where it is based on a few-body eikonal approach. Tostevin[119] has proposed a modified spectator core model for the calculation of partial cross sections to definite final states of the surviving core fragment.

Considering first the simple case of a two-cluster (core+n) projectile interacting with a target, the total cross section for stripping of the neutron and detecting the surviving core (c) in a particular final state, J_c^π (spin J_c and parity π), can be written as

$$\sigma_{st}(J_c^\pi) = \frac{1}{2J+1}\int d\mathbf{b}\sum_M \langle \Phi^c_{JM}|\ (1-|S_n(b_n)|^2)\ |S_c(b_c)|^2\ |\Phi^c_{JM}\rangle\ , \qquad (35)$$

where Φ^c_{JM} is the ground state wave function of the projectile, with angular momentum J and projection M, containing the core fragment in state J_c^π. This is thus only part of the projectile's total ground state wave function which may well contain contributions from configurations involving different core states. Note that Eq. (35) is essentially the same as Eq. (33) only here the cross section is just that part of the full stripping cross section in which the spectator core is in the state J_c^π both before and after the stripping process.

As an example of the procedure we present the case for the (^{16}C,^{15}C) [120] in figure (13). The momentum distribution for the outcoming ^{15}C are measured along with any coincidence γ-rays from the decay of excited core states, allowing the extraction of a spectroscopic factor and angular momentum from the overall normalisation and the shape of the distribution.

When dealing with a three-body projectile involving a core and two valence neutrons, the surviving fragment in equation (35) (i.e. after the removal of just one of the neutrons) is now itself a composite system of core plus neutron, which may be loosely-bound. To check whether the spectator core assumption remains valid in this situation, a four-body generalisation of the Tostevin model, that allows for the dynamic coupling of different fragment states in the stripping process, was developed [121] and applied to a number of reactions such as ^{9}Be(^{12}Be,^{11}Beγ) at 78 MeV/A. For this reaction, partial cross sections to both the $\frac{1}{2}^+$ ground state and $\frac{1}{2}^-$ first excited state of ^{11}Be have been measured and calculated [122]. It is known that only one third of the ground state wave function of ^{12}Be (which is treated as a three-body (^{10}Be+2n) system [123]) comes from a closed p-shell configuration, with the valence neutron pair spending most of their time in the $(1s^2+0d^2)$ intruder configuration. Clearly, the $s_{1/2}$ intruder ground state in ^{11}Be has some effect on the configuration mixing in ^{12}Be. However, the spectroscopic factors deduced from the cross sections estimated in the Tostevin spectator model will

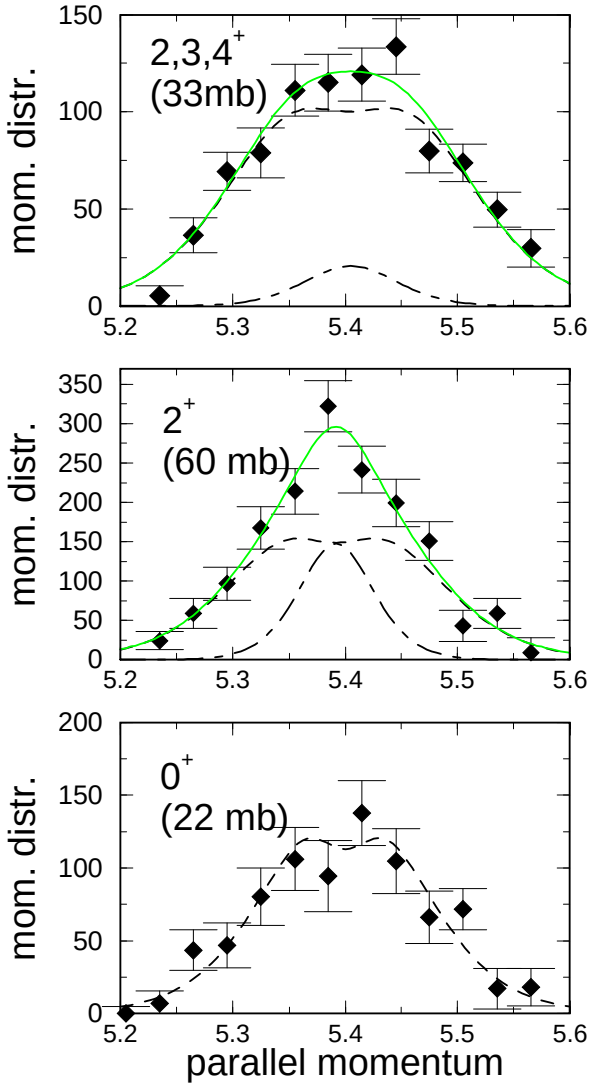


Figure 13. Partial longitudinal momentum distributions corresponding to the states in the simplified level scheme of ^{16}C. The bottom panel corresponds to populating the g.s., the middle panel to the 2^+ state at 1.77 MeV and the top panel to the bunch of three states all around an excitation energy of ~ 4.1 MeV. The data is from [120].

be modified if dynamical coupling between the different ^{10}Be+n states ($1s_{1/2}$, $0p_{1/2}$ and $0d_{5/2}$) in the projectile and the bound states ($1s_{1/2}$ and $0p_{1/2}$) of the final ^{11}Be are important.

It was found [121] that allowing for couplings between different single particle states caused a less than 10% overall increase to the stripping cross section. Such a correction gives an indication of the reliability of the spectator assumption and suggests that it is better than might be expected for such a 'core' as ^{11}Be. Similar modifications to the partial stripping cross sections have also been found when applied to the reaction (^{16}C,^{15}C), where the knockout cross sections to the $\frac{1}{2}^+$ ground state and $\frac{5}{2}^+$ excited state of ^{15}C have been measured [120]. In this case, including the dynamical coupling

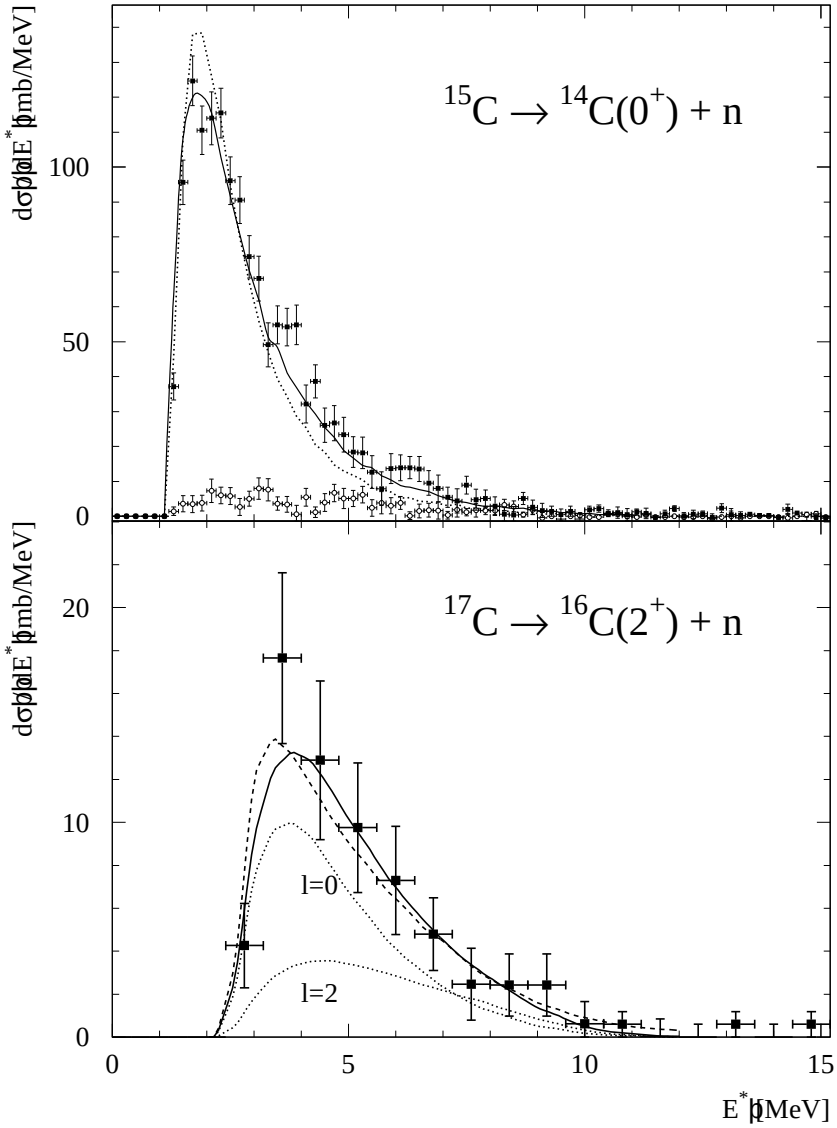


Figure 14. Differential cross sections for Coulomb dissociation with respect to excitation energy, E^* of ^{15}C and ^{17}C on a lead target at beam energies of 605 and 496 MeV/nucleon, respectively [124]. See text for details of the different curves.

between different single particle states of the valence neutron in ^{15}C give rise to an overall *reduction* in the stripping cross sections. The changes are nevertheless relatively small (of order 5%).

It should be emphasised that there are other effects which, if included, could also affect the calculated cross section, such as core recoil, the use of a more realistic three-body wave function for the projectile and, maybe most importantly, including collective core excitation effects in both the initial and final wave functions.

Another way of studying the single particle structure of exotic nuclei is via Coulomb dissociation at fragmentation energies of several hundred MeV per nucleon. Using the same technique as developed by the MSU group on knockout reactions, experiments at

GSI also measure the decay neutron and any γ-ray in coincidence with the projectile. The differential Coulomb dissociation cross section, $d\sigma/dE^*$, is then the incoherent sum of components corresponding to the different core states populated following the removal of the neutron. Figure (14) shows such cross sections for the dissociation of both ^{15}C and ^{17}C into ^{14}C and ^{15}C, respectively. In both graphs, the solid curves are the result of a direct breakup model using a plane wave approximation [124]. The dotted curve in the upper graph and the dashed curve in the lower graph both correspond to a distorted wave approximation analysis.

Many of the techniques to describe one or two nucleon knockout reactions as a spectroscopic tool for studying dripline nuclei are still under development. For example, when the surviving fragment is a halo state, whereas it was more tightly bound within the projectile (prior to the knockout of a valence neutron), it is necessary to include an overlap (or 'mismatch') factor due to the change induced in the remaining valence neutrons binding energy. Since this field is relatively new, it is not appropriate to discuss it further in this review. However a recent review of the work in this area can be found in ref.([125]).

7. Transfer reactions

The history of transfer reactions with radioactive beams for studying the structure of exotic nuclei is a relatively recent one. Thus there have not been many specific developments of transfer theories with the aim of dealing with halo-like nuclei. We will here present the few applications that have been performed with conventional methods and discuss the additional developments that have been proposed.

7.1. DWBA

Traditionally, DWBA (Distorted Wave Born Approximation) has proved to be extremely useful to extract spectroscopic information in Nuclear Physics, thus one can find it in most text books [126]. As it retains only the first term of the Born series, the transfer process is performed in one step. One needs to determine the initial and final distorted waves describing the relative motion of projectile and target. The intrinsic structure information is contained in the spectroscopic factor, and multiplies the full DWBA cross section. This factor can then be related to the structure information calculated in microscopic models [127].

In DWBA, the transition matrix element for the transfer reaction $A(X,Y)B$, where $A = B + v$ and $Y = X + v$, can be written in post form,

$$M^{post} =< \Psi_f^- \; I_{YX} \mid V_{vB} \; + \; V_{BX} - U_{BY} \mid I_{AB} \; \Psi_i^+ >, \tag{36}$$

and in prior-form

$$M^{prior} =< \Psi_f^- \; I_{YX} \mid V_{vX} \; + \; V_{BX} - U_{AX} \mid I_{AB} \; \Psi_i^+ > . \tag{37}$$

Here, $I_{AB} = \phi(r_{v-B})$ is the overlap function of the composite nucleus A and its core B, and $I_{YX} = \phi(r_{v-X})$ is the overlap function of the composite nucleus Y and its

core X. The distorted waves Ψ_f^-, and Ψ_f^+ are calculated using the corresponding optical potentials U_{BY} and U_{AX}. Often the remnant term in the transition operator ($U_{rem}^{post} = V_{BX} - U_{BY}$ or $U_{rem}^{prior} = V_{BX} - U_{AX}$) is neglected. Furthermore, the zero range approximation may be applicable to either V_{vB} or V_{vX}.

Even when applied to reactions with stable beams, the DWBA was considered to have a limited accuracy ($\approx 30\%$). One of the reasons for this restriction is due to uncertainties in the optical potentials responsible for distorting the incoming and outgoing waves. Typically, one makes use of elastic scattering data taken over a wide angular range, to pin down the optical parameters. With radioactive beams, these data are not available, and in some cases even not measurable. So far, in most applications to exotic nuclei, optical potentials have been obtained via several methods: either extrapolated from nuclei in the valley of stability (global parametrisations), or from double folding models involving projectile and target densities, or have been determined with elastic data taken only at forward angles, where the sensitivity to the parameters is low [128]. As a consequence, these optical potentials may bring about large uncertainties [129].

In addition to the distorted waves, one also needs to worry about the transfer transition operator. So far results show that zero range DWBA should not be used for halo nuclei. Also, the core-core interaction for these dripline nuclei may differ significantly from the potential describing the scattering of the unstable nucleus from the target. Then there is no cancellation of the remnant term in the transfer operator. For loosely bound systems, finite range effects, as well as the remnant contribution, have been shown to be important [129].

Often the cores of dripline nuclei are stable and can be used as targets. In those circumstances stripping reactions can populate states of the exotic nucleus, thus providing some spectroscopic information. However, in order to get the full spectroscopy of the ground state the exotic nucleus should be used as the beam.

The initial attempt to extract the structure of an exotic nucleus using a transfer reaction was for ^{11}Be through a (p,d) reaction in inverse kinematics [130]. Being the first of what we expect will be a series of experiments, it is important to understand the approximations performed in the calculations used for the analysis of the data, and identify the accuracy of the approach.

First, let us review briefly what is known about the ground state structure of ^{11}Be. It is well accepted that the loosely bound neutron is mainly in an $s_{1/2}$ state, but there is also a significant core excited ^{10}Be(2^+) component, where the neutron is found in a $d_{5/2}$ state. In [130] these components are initially calculated separately, and added incoherently, in the Separation Energy prescription. Keeping in mind that the deformation of the core is very strong in this system, dynamical effects are bound to play a role. In such cases, the components for the ground state wavefunction should be calculated properly, in a coupled channel description.

Secondly, the choice of optical potentials needs to be considered. The proton optical parameters are taken from proton elastic scattering data of stable nuclei, and there is no

evidence that this is a correct procedure. Although the deuteron-^{10}Be elastic scattering has been described at nearby energies with the optical model, there is the possibility of the deuteron breaking up in the process. Then the ADBA potential (Adiabatic Deuteron Breakup Approximation) may be more adequate [17]. Note that adiabatic models were discussed in section 2.3. The difference between these two potential choices is considerable. Unfortunately, the transfer cross sections are very sensitive to the parameters of both entrance and exit potentials. It seems that only additional elastic and breakup data, taken exactly at the relevant energies, would reduce all these uncertainties.

Similar concerns on the possible inadequacy of the optical potentials could be expressed for the extraction of spectroscopic factors for ^{17}F, from the analysis of ^{16}O(d,n) data [131].

The ANC method offers an indirect measurement for the low energy capture rates needed in astrophysics, through transfer reactions. DWBA is widely used in the extraction of ANCs (Asymptotic Normalisation Coefficients) [132]. The essential condition for the applicability of the ANC method is that the reaction should be completely peripheral, so it will only probe the asymptotic part of the overlapping wavefunctions. The applications have concentrated on ^{8}B [133], although there are many ongoing projects to measure ANCs for other loosely bound nuclei. Essentially, there have been two independent sets of measurements: those on the very light targets, i.e. (d, n) and (^{3}He,d), or those on heavier targets (typically the stable Boron to Oxygen isotopes). In (d, n), even if the reaction is peripheral, the transfer cross section depends very strongly on the choice for the optical potentials, and typically elastic scattering corresponding to the exit channel cannot help in pinning down the parameters [129]. In addition, deuteron breakup may need to be considered. For heavier targets, the dependence on the optical parameters is not so strong, but there are many open channels accessible to the reaction path. Other tests of the validity of the DWBA approach should then be performed. This discussion will continue in the following section.

For three body projectiles, the partial wave decomposition involves the coupling of four angular momenta and a converged calculation can easily become unfeasible. In [134], the partial wave decomposition is avoided by performing the nine-dimensional integral corresponding to the DWBA transition amplitude [134]. Results for two nucleon transfer of 151 MeV ^{6}He on proton and alpha particles are extremely promising. By including the three-body structure into the reaction calculation, this work shows how the details of the halo ground state are determinant in the reaction process.

7.2. Coupled channels

There are many ways of going beyond the one-step DWBA approach, and we shall mention a few here.

If there are strongly coupled open inelastic channels in the entrance (exit) partition, one can still treat the transfer process in first order, but allow for various steps between the relevant entrance (exit) channels. This provides an n-step DWBA method which

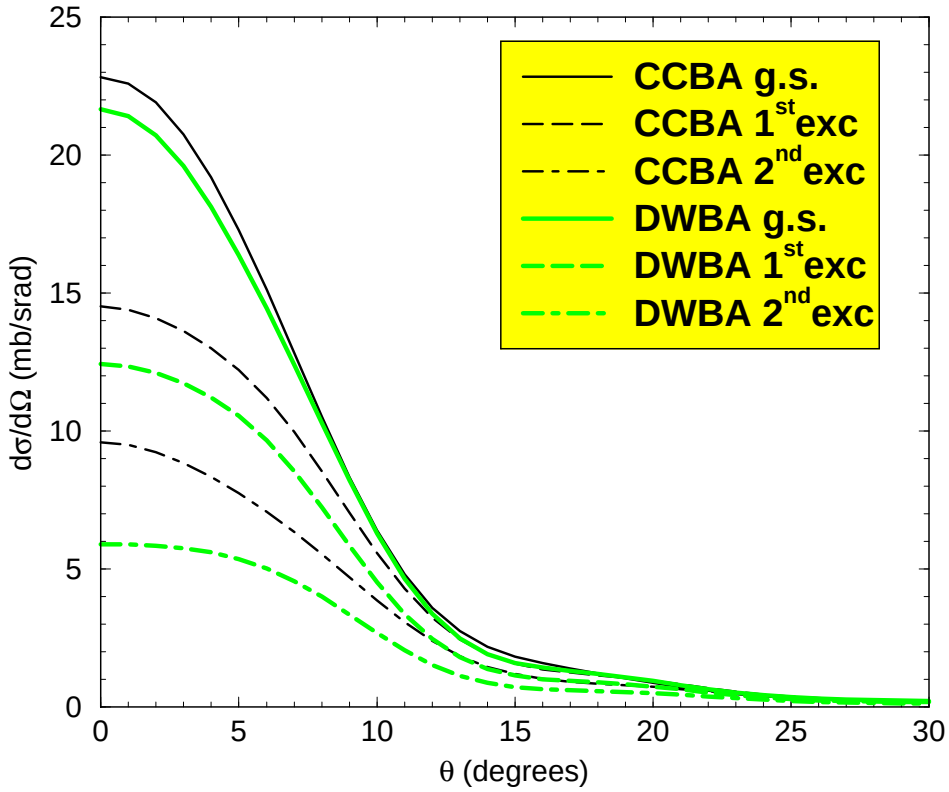


Figure 15. The transfer cross section for ^{10}B(^{7}Be,^{8}B)^{9}Be at 84 MeV: grey lines are the result of DWBA calculations whereas black lines are those for CCBA.

becomes the CCBA method (Coupled Channel Born Approximation) when the inelastic couplings are treated to all orders.

Intuitively one would guess that transfers on well deformed targets require a CCBA reaction model instead of the DWBA, as inelastic couplings are known to be strong. This was confirmed by the coupled channel tests performed in [135]. In figure (15) the transfer to the three first states in ^{9}Be are predicted. The differences between the grey lines and the black lines gives an estimate of the error made when using the one-step approach.

Alternatively, one can also have couplings within the radioactive projectile, due to inelasticities of the core. There should obviously be consistency in the structure and the reaction models used. If the structure model predicts, as in the case of ^{11}Be, a significant core excited component, then core excitation needs to be included in the reaction model through an n-step DWBA or preferably a CCBA formalism. The large two-step DWBA contribution to the ^{11}Be(p,d) reaction estimated in [130] does not come as a surprise.

One should still consider the proximity to threshold of these exotic projectiles. This may provide strong couplings to the continuum which in principle can affect the transfer process. As mentioned before, breakup cross sections for these nuclei are generally large and may feedback to the transfer cross sections. In such cases, one of the standard theoretical approaches to handle the problem is the so-called CDCC-BA method, where the continuum is appropriately discretised and fully coupled, but the transfer process is

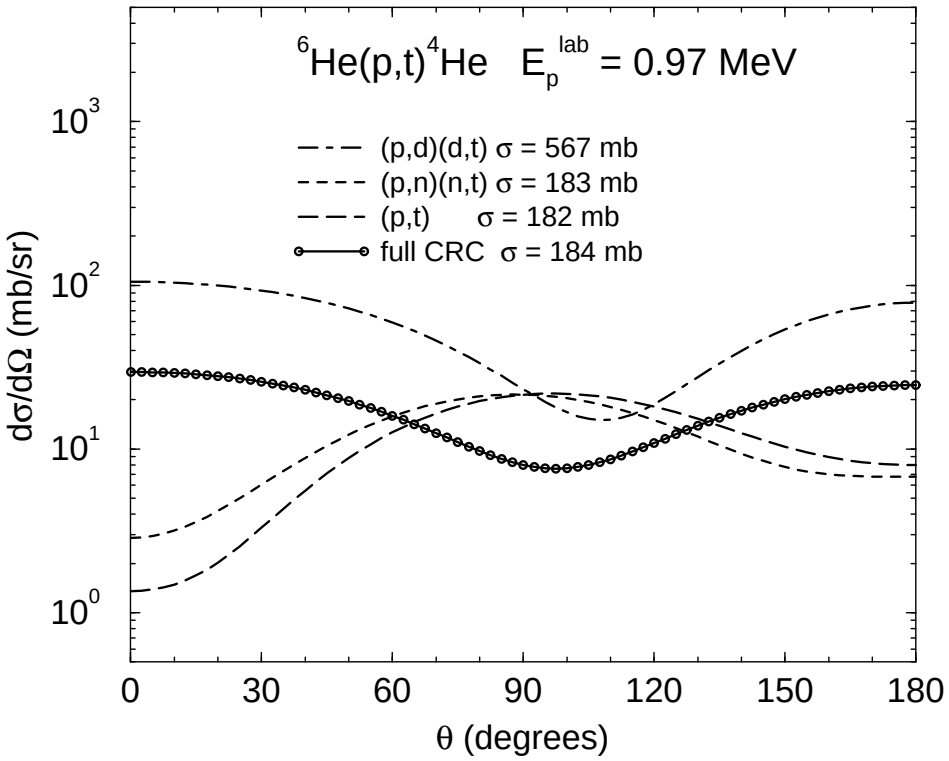


Figure 16. The 2-nucleon transfer of ^{6}He on protons.

still treated in first order Born approximation. CDCC-BA calculations were performed for the reaction ^{14}N(^{7}Be,^{8}B)^{13}C [136, 137] and the results show that for this system, the transfer is not affected by couplings to the continuum, in particular in the forward angle region.

The complexity of the problem increases when there is the possibility of breakup in both entrance and exit partitions, such as is the case for ^{7}Be$(d,n)^8$B. The first attempt of including both deuteron and ^{8}B breakup in this reaction was presented recently [138] although many approximations were involved in the simplified version of the CDCC-BA-CDCC model. In these calculations, the basis is over complete, and orthogonality issues need to be carefully considered. Also, such a calculation sits at the limit of computational capacities. In spite of this, more calculations along these lines will be needed in the future.

If the transfer is very strong, then first order Born series may not be sufficient. One can then allow for multi-step transfer through the CRC (coupled reaction channels) method. Applications to transfer reactions with ^{11}Be [130] and ^{8}B [129] show that such higher order multi-step terms provide less than 10% corrections.

When more than one nucleon is transferred, one-step transfer may be supplemented by two- and higher order step-processes. When the reaction time is large, the system can rearrange itself in several ways. Inevitably one can find many transfer paths for the

reaction, which need to be coupled in a CRC method. The low energy experimental program using the ^{6}He beam in LLN [139] motivated the application to ^{6}He+p [140]. In figure (16) the various multistep paths relevant to the reaction are shown as well as the total cross section, resulting from the interference of the considered channels. Calculations were performed within a CRC formalism. In those calculations, one and two-nucleon transfer form-factors were determined within a three-body structure model and a full finite-range treatment was included. Both the remnant term and nonorthogonality corrections were found to be necessary. Couplings to all open channels were important to generate the final cross sections.

7.3. Other methods

When the transfer process occurs at sufficiently high energy, a Glauber approach is possible [141]. The sensitivity to details of the projectile wavefunction is shown to be very strong in the calculations for ^{11}Be$(d,p)^{10}$Be, although only a single particle form factor is assumed. In fact, one expects that the sensitivity is more on the scale than the shape details and components. It would be interesting to confirm this by improving the structure information included in the reaction model.

If, on the other hand, the energy is not very high, but still high enough compared to the binding energy, an adiabatic approximation can be safely made. An adiabatic model was developed for one-nucleon halo nuclei [142]. The T-matrix is written so that only the halo-nucleon/target interaction appears in the operator. Then both core-halo and target-core interactions need to be considered in calculating the entrance(exit) wavefunction. The adiabatic solution is a distorted wave that includes recoil and breakup effects (REB). The exact wavefunction appearing in the exit(entrance) channel is approximated to a distorted wave and the adiabatic limit is also taken (making use of the Johnson-Soper potential [17]). Calculations for ^{16}O$(d,p)^{17}$F, ^{10}Be$(d,p)^{11}$Be and ^{11}Be(p,d)^{10}Be are presented. The REB effects generally increase the cross section, so that the extracted spectroscopic factors are generally reduced. In all cases the impact of deuteron breakup on the transfer cross section was stronger than that of the heavier nucleus. The example for ^{11}Be(p,d) populating both the g.s. and the first 2^+ in ^{10}Be is shown in figure (17). Disappointingly, the spectroscopic factors extracted for ^{11}Be g.s. do not agree with those in [130], although a direct comparison with this data was not performed. It would be interesting to include core excitation in this reaction model, as the d-wave dynamics are expected to change the picture. Also, a comparison with the various standard models is necessary to better understand the advantages and drawbacks. Nevertheless this model is very promising, since in principle it can deal with breakup in both entrance and exit partition and yet is not computationally demanding.

Sometimes, transfer methods can be applied to breakup reactions. The usual way to think about projectile breakup ($P \Rightarrow C + x$) is as $T(P, C + x)T$. However, the transfer to the continuum of the target $T(P, C)T + x$ is formally equivalent to this, and the calculation may converge more quickly. If the experiments cannot distinguish

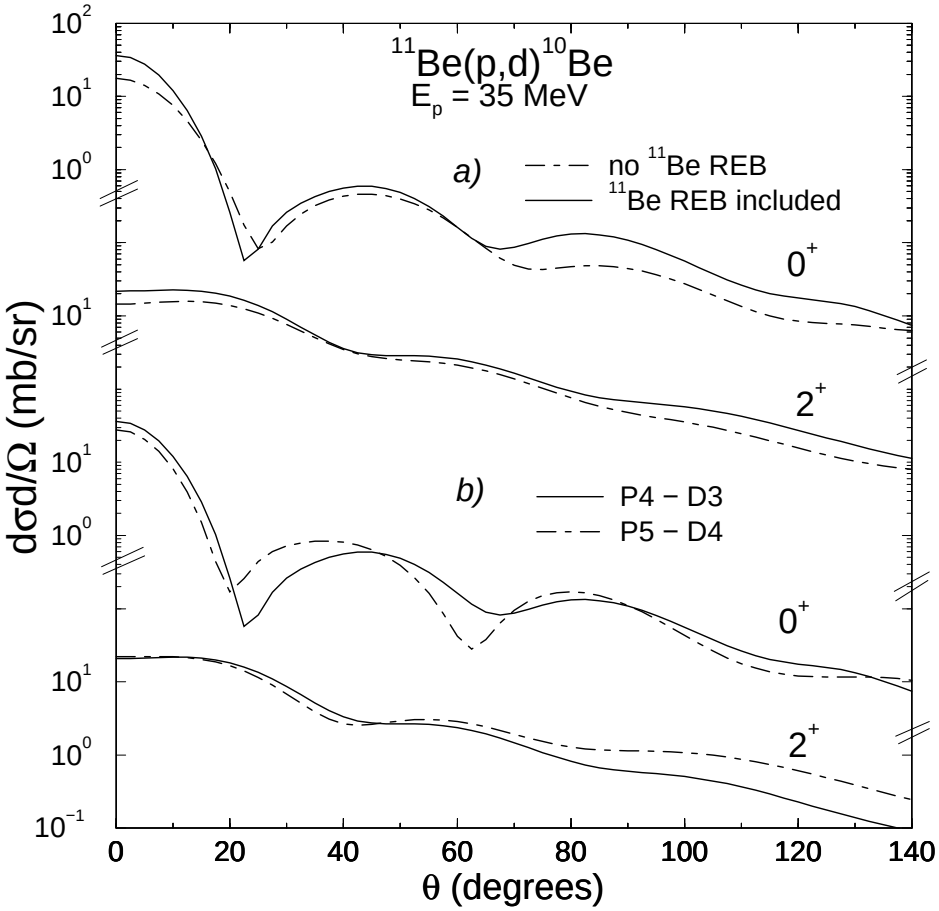


Figure 17. The transfer reaction ^{11}Be(p,d)^{10}Be($0^+, 2^+$): a) comparing the effect of REB for a fixed set of optical potentials; b) comparing two choices of optical potentials while including the REB effect. In both cases the deuteron breakup was included.

the two processes apart, then the transfer description (including bound and unbound states) may become more attractive. This approach offers the best description to date of the ^{6}He 2n low energy transfer/breakup on ^{209}Bi [99]. It is also proving to be very promising for the ^{8}Li transfer/breakup on ^{208}Pb [143].

8. Fusion

Theoretical developments for fusion reactions, specifically designed for light dripline nuclei, are still scarce, partly due to the fact that accurate fusion data on these nuclei is rather recent, and partly because fusion makes up such a small fraction of the reaction cross section. For this reason we first point out a few general aspects concerning the theory of fusion reactions with stable nuclei, of relevance for loosely bound systems, and discuss the theoretical advances when applied to RNBs.

8.1. Some relevant ideas from Heavy-ion fusion

It was only in the early eighties that the heavy-ion fusion data allowed the refinement of fusion calculations, which now go much beyond the basic barrier penetration ideas [144], and incorporate coupled channel effects of various types (e.g. [145, 146, 147, 148, 149, 150]). There are essentially two approaches: a) the fusion process is modeled with a strong imaginary potential in the interior, taking into account the loss of flux from all other channels and b) the incoming boundary condition method, where each component of the wavefunction is matched to an incoming wave on the barrier. In both cases a coupled channel equation is solved. The first approach generally contains very strong imaginary potentials which remove any couplings acting in the barrier region. Under these circumstances, as couplings are limited to larger distances where they are typically weaker, the DWBA first order solution may be adequate to describe the mechanism. However, in the strong coupling limit, the determination of the imaginary potential is by no means transparent and coupling effects may be misinterpreted [146]. It is often preferrable to use the incoming boundary condition, both for technical and physical reasons. Often one also takes the adiabatic approximation, when excitation energies of the colliding nuclei are negligible compared to the fusion energy, and the differences in the centrifugal barriers can be ignored [149]. Lindsay *et al.* [149] showed that, in the strong coupling limit, the adiabatic calculations reproduce the full coupled channel results, while the DWBA calculations overestimate the fusion cross section. Explicit simplified expressions in terms of the one channel cross section have been deduced for vibrational and rotational structures [149].

It is well understood that in general the inclusion of extra channels, coupled into the reaction mechanism, produce more steps in the barrier distribution and consequently spread the energy range over which the transmission factor goes from zero to unity. This produces enhancement of sub-barrier fusion, and hinders fusion above the barrier [146, 149].

Also, while the flux transmitted by the barrier in a particular channel (fusion) depends on the strength of the interaction through the barrier, the reflected flux, the reaction cross section that is experimentally seen, depends on the couplings outside the barrier. This means that the connection between the fusion part and reaction part of the flux for each channel is not straightforward.

It has been shown that the energy matching for the channel to be coupled, relative to the incident channel, is a crucial ingredient. In fact, negative Q-values tend to reduce the relative enhancement of sub-barrier fusion (when comparing with the perfectly matched channels Q=0), and positive Q-values tend to enlarge these effects [146, 147]. However, negative Q-values produce an increase of the overall fusion flux and positive Q-values an overall decrease, when compared with $Q = 0$.

The inclusion of inelastic couplings alone is frequently not enough to describe the data [148, 151] and transfer couplings have been suggested as the necessary solution. Neutron transfer has often been a successful explanation for the enhancement of sub-

barrier fusion cross sections (see for instance the results on the fusion of ^{58}Ni+^{64}Ni, relative to ^{58}Ni+^{58}Ni [145]). One can expect that for loosely bound neutron rich (or proton rich) nuclei this effect will become even more important.

Given the influence of both inelastic couplings and transfer couplings, fusion calculations can easily become rather demanding. The CRC method (coupled reaction channels) mentioned in section 5 offers a reliable path for the fusion calculation [150]. In the end, a consistent description of the elastic, inelastic and transfer channels should be obtained, at the same time as the fusion cross section.

The number of data sets on the fusion of light dripline nuclei is increasing by the day, yet we are still far from understanding the general behaviour [152]. Given the importance of breakup and transfer channels, experiments designed to measure specifically these components have been carried out (e.g. [99]). Nevertheless, many studies are still presently performed on the stable Li or Be isotopes, where systematic trends can be more easily identified [153]. Below we discuss the theoretical contributions in this field, starting with the simple models initially used, up to the full CDCC or the time-dependent models, already applied in earlier sections.

8.2. Preliminary fusion results

Interest in the fusion of dripline nuclei was initiated in the early nineties for two reasons: to better understand the exotic properties of these nuclei and for the hope of insight into the production of the superheavy elements. The first sequence of theoretical work was applied to ^{11}Li [154, 155, 156] for which there are as yet no available data.

In [154], a two-channel fusion calculation included a resonance at around 1.2 MeV (referred to as a pygmy resonance, or giant dipole resonance). The possibility of breakup was accounted for through a survival probability multiplying factor. The idea was that breakup channels take flux away from fusion. Even though rather poor, the adiabatic approximation was used. The conclusion was that fusion is suppressed above the barrier, and the prediction of sub-barrier enhancement is lower than what would be obtained if no breakup was included. It was subsequently pointed out that the breakup channel need not reduce fusion [155]. In fact, the additional coupling could produce enhancement in the same way inelastic or transfer couplings do. The coupled channel calculations in [155] determine the complete fusion of ^{11}Li on ^{208}Pb for the same barrier parameters as those used in [154]. Results show enhancement due to the dipole coupling and further enhancement due to the coupling to breakup states. A theoretical improvement of the treatment of resonant channels in [154] uses doorway states [156]. The results confirmed fusion hindrance around the barrier, sustaining the controversy.

As knowledge of the properties of light exotic nuclei increased, breakup and transfer channels became an unavoidable issue when considering the fusion process. Many of these nuclei do not have excited states and the inclusion of inelastic excitation of the target is by now a standard procedure. However, given the loosely bound nature of these beams, the coupling strength to continuum channels is expected to be strong and

the Q-value for neutron transfer (for neutron rich) or proton transfer (for proton rich) can become positive, which if well matched can also produce strong coupling.

In [157], a study of the effect of transfer and inelastic couplings on the fusion of ^{11}Be+^{12}C is performed. The CRC calculations included both bound states and the d-wave resonance of ^{11}Be, as well as several one-neutron transfer channels to ^{10}Be+^{13}C, corresponding to the three first states in ^{13}C and the first two states of ^{10}Be (note that all have positive Q-values). The equations were solved using a strong but short-range imaginary potential in order to remove coupling from small distances. It was found that the transfer alone decreases the fusion and that inelastic couplings partly compensate this reduction. Coupling effects dissappear at higher incident energies while the maximum effect is found just below the barrier.

8.3. The time-dependent method

One can also determine the fusion cross section using the time evolution of a wavepacket, solution of the time-dependent Schrödinger equation. Such calculations were performed by Yabana [158] for a core+n system impinging on a target, that simulates the ^{11}Be+^{40}Ca reaction. Due to computational limitations, nuclei are considered spinless, only l=0 relative motion is included, and the wavepacket is confined to a finite radial region where only the Coulomb part of the core-target interaction is felt. The absorption is included through the imaginary part of the core-target interaction alone, thus the fusion cross section contains both complete and incomplete fusion. The behaviour of the process for low binding (-0.6 MeV) is compared with a system with stronger binding (-3 MeV). Breakup, transfer, and fusion cross sections are simultaneously calculated.

It was found in that study that, by increasing the depth of the neutron-target potential until binding is larger than the binding of the neutron in the projectile, the projectile-target kinetic energy is increased, producing an increase of the fusion cross section. The opposite effect happens when the n-target interaction produces less binding for the n-target system than the separation energy of the neutron in the projectile. However, when the projectile binding is already very low, the likelihood is that the neutron will have a larger binding to the target, resulting in an overall suppression of fusion. Fusion cross sections as a function of beam energy show a slight enhancement below the barrier and a clear reduction above the barrier.

8.4. The CDCC method

The CDCC method is another possibility for including breakup effects when calculating the fusion reaction. In the CDCC calculations for the fusion of ^{11}Be and ^{208}Pb performed by Hagino *et al.* [159], several truncations are made in order to concentrate on pure breakup effects (results are shown in figure 18). Continuum-continuum couplings are ignored, as well as projectile and target inelastic excitations. The neutron in the projectile is assumed to be in a pure $2s_{1/2}$ state and only transitions to $p_{3/2}$ are considered. The incoming boundary condition method is used for solving the coupled

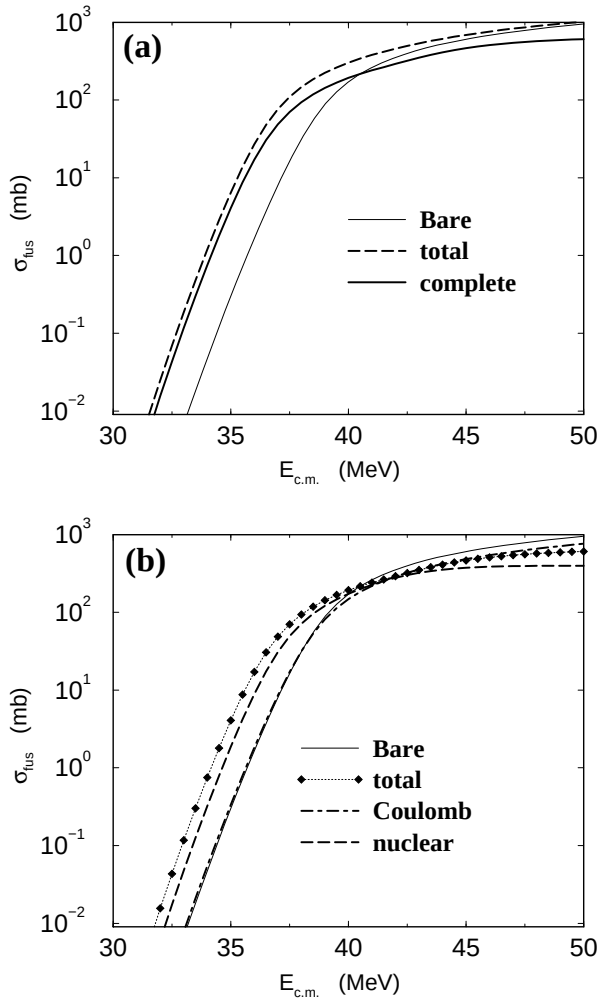


Figure 18. The fusion cross section for ^{11}Be+^{208}Pb as a function of bombarding c.m. energy: (a) complete fusion (thick solid) and the total fusion (dashed) are compared with the simple penetration model (thin solid); (b) the nuclear (long-dashed) and Coulomb (dot-dashed) contributions to the complete fusion (diamonds). The barrier penetration model is shown (thin solid) for comparison.

channel equations, and the isocentrifugal approximation is made. The results predict fusion enhancement below the barrier and suppression above the barrier, in agreement with the early results of [146]. The dynamical effects of the couplings are essential. It is shown that the coupling form factors at around barrier distances, peak at relatively large energies, behaving in a completely different way than the asymptotic coupling form factor. The same conclusions were obtained for the fusion of ^{6}He and ^{238}U for an identical calculation [160].

More recently a full CDCC calculation, without the above mentioned truncations, was performed in order to calculate the fusion of ^{11}Be and ^{208}Pb [161]. Although inelastic excitations of the target and transfer couplings were left aside, the calculation included the projectile excited state $1/2^{-}$ as well as all multipoles in the continuum

needed for convergence. The fusion cross sections were defined in terms of a short-range imaginary potential. It was found that the excited $1/2^-$ state of ^{11}Be has little influence on the fusion, redistributing the fusion cross section. If no continuum-continuum couplings were included, the conclusions of [159] for complete fusion were corroborated: strong enhancement below the barrier and hindrance above the barrier. However, since incomplete fusion is relatively large above the barrier, the total fusion cross section, for this energy region, was not reduced, when compared with the no-couplings case. The truly surprising result was the effect of continuum-continuum couplings: the reduction of the complete fusion cross section was of nearly two orders of magnitude in the sub-barrier region and around an order of magnitude above the barrier. In addition incomplete fusion is also reduced. This means that the sub-barrier enhancement is much weaker, for the complete and total fusion processes and there is suppression above the barrier for both complete and total fusion.

Note that, in [161], complete fusion is associated with absorption from the bound channels only, when in principle it is possible that the projectile suffers complete fusion even after breaking up. Also, incomplete fusion is associated with absorption from the breakup channels, and so the real incomplete fusion could be lower than that calculated in [161]. Nonetheless, the total fusion cross section is unambiguous and can be compared with experiment. Agreement is found below the barrier but cross sections are underpredicted above the barrier.

A better understanding of the role of the continuum-continuum couplings is probably necessary to be able to improve the theoretical description. In addition, the separation of complete fusion from incomplete fusion in both the data and calculations would also be helpful. Given the conclusions in [157], transfer channels will inevitable need to be included in a CDCC-CRC type calculation before a definite conclusion can be drawn, albeit the calculations presented in [161] were already at the limit of our best computational possibilities. At present, the extraction of structure details from fusion data seems to be unlikely. Notwithstanding, it still offers one of the best alternatives to learn more about the production of superheavy elements.

9. Charge exchange and photonuclear reactions

Another way to study the structure (both bound state and continuum) of exotic nuclei is through charge exchange reactions. However, where measurements have been made for (n,p) reactions, for instance ^{6}Li$(n,p)^6$He [162] and ^{14}Be$(n,p)^{14}$B [163], the experiments have suffered from poor statistics and energy resolution such that individual final states could not be resolved. Alternatives to this are the $(t,^3$He) and (^{7}Li,^{7}Be) reactions. The reaction ^{6}Li$(t,^3$He$)^6$He has been studied at MSU [164] and the continuum structure of ^{6}He probed. However, little theoretical work has been carried out. Ershov and collaborators [165] have studied the ^{6}Li$(n,p)^6$He within a four-body DWBA model and also point out that ^{6}He$(p,p')^6$He is a useful complimentary probe. A few-body eikonal model for charge exchange has been developed by the Surrey group but has so far been

applied only to the $(d, 2p)$ reaction [166].

In recent years, there has been a growing interest in the use of charged pion photoproduction reactions, $(\gamma, \pi^{\pm})$, as a tool for studying nuclear structure. In particular, because of recent advances in intermediate energy "electron" factories, and the development of high resolution pion spectrometers, precise angular distributions for the produced pions can be measured and, it is anticipated, individual final states of the nucleus of interest can be resolved. As discussed in this review, most of what is known about exotic nuclei has been obtained through fragmentation reactions in which the strong interaction, particularly that of the core, plays a major role. Pion photoproduction studies offer an alternative, cleaner, electromagnetic probe of nuclear structure. In such charge exchanging reactions (e.g $^{6}\mathrm{Li}(\gamma, \pi^{+})^{6}\mathrm{He}$) the pion energy and momentum can provide information about the valence nucleon participating in the reaction $\gamma N \rightarrow \pi N$.

A major advantage of such reactions is that they can probe the entire nuclear wavefunction, unlike the surface-dominated fragmentation reactions which tend to only probe the wavefunction tail. Of course, depending on the momentum transferred in the process, such reactions can also probe the surface and be used to study the halo, without ambiguities due to any core potential. Karataglidis *et al.* [167] have carried out a DWBA calculation in which the nuclear transition density is obtained using the shell model, in a similar way to the group's studies of proton elastic and inelastic scattering [58].

Several years ago it was suggested [168] that excited state halos can also be probed in this way. It was shown that the pion cross sections calculated for the $^{17}\mathrm{O}(\gamma, \pi^{-})^{17}\mathrm{F}(\frac{1}{2}^{+}$,0.495 MeV) reaction is sensitive to the halo structure of the valence proton.

Finally, an alternative photonuclear probe that does not involve charge exchange is via the (γ, p) reaction. Boland *et al.* [169] have observed a broad resonance in the ^{6}He continuum at 5 MeV but are unable to define its exact nature. Such reactions are in need of further theoretical analysis as well as more accurate measurements.

10. Outlook

In this review we have attempted to cover many theoretical aspects concerning reactions with light dripline nuclei, paying particular attention to the interplay between the structure input and the reaction model. In order to obtain a successful description of the reaction, specific features associated with the exotic nature of these nuclei need to be included. Furthermore, as data becomes more detailed and accurate, better models are required. Better models typically imply that calculations become larger and new numerical methods need to be developed in order to ensure progress in the field. Given some discrepancies found between theory and experiment, the suggestion that core excitation can dynamically interfere in the process needs to be checked. Improvements to the single particle models, extensively used to date, are then necessary to assess

the role of core excitation in the reaction mechanism. Finally we comment on possible physics with electron beams.

10.1. Continuum couplings and computation

Continuum coupling is crucial for understanding certain reaction processes involving light exotic nuclei. These coupling effects are best seen in breakup processes, but it has also been shown that there is an important influence on elastic scattering and fusion reactions. In fact, the results on fusion are so large that they call for further investigations. Couplings to the continuum may be less important for transfer reactions and certainly more examples need to be analysed before any general statement can be made.

When including continuum coupling in a reaction model, one should definitely take care of the non-resonant continuum as well as resonant states. Couplings between two continuum states may be equally (or even more) important as couplings between the ground state and the continuum. Many results discussed here use the well established CDCC method to discretize the continuum. However, given the computational demand of the traditional CDCC calculations, new methods are being developed. One of the most promising alternative methods for discretizing the continuum uses transformed harmonic oscillators (THO). Benchmark calculations comparing the CDCC and the THO methods for the elastic scattering and breakup of deuterons on ^{208}Pb are very encouraging [171]. We expect that, in the future, the optimization of the continuum discretization will make it feasible to tackle reactions involving three body systems, such as ^{11}Li, by including the three body continuum properly.

On the same lines, the very recent work presented in [**?**] proposes a pseudo-state discretization using real and complex-range Gaussian bases to calculate the breakup within the 3-body CDCC picture. Applications to the 4-body CDCC problem are also under consideration.

10.2. Core excitation

In recent years, the description of light exotic nuclei based on single particle models has become unsatisfying. Although extremely attractive for their simplicity, one needs to go beyond the inert core approximation in order to account for the physics that can now be accurately measured in the new facilities. We have already mentioned the experiments involving the Be isotopes, where excited core components were clearly identified (e.g. [122, 130]). Evidence for a core excited component was also found in the breakup of high energy ^{8}B [172]. Besides, similar results are to be expected for many other nuclei.

In the light of these new experimental results, theoretical reaction models need to encompass core excitation. As excited states of the core involve typically larger angular momentum, there will be a rapid increase of the number of available reaction channels. In cases such as ^{8}B where the ground state of the core is a $3/2^{-}$ state, the spin of the core has been routinely neglected and most models do not allow the core structure to

play any role in the reaction mechanism. In reaction models that include core excitation, this can no longer be done and the calculations become much larger. Apart from the computational demands, there are some theoretical issues that need to be addressed. Namely, since the loosely bound systems often require the coupling to breakup states, a reaction model with core excitation implies that both bound and unbound states need to have core excited components. It is thus necessary to generalize the CDCC approach to include core excitation within the projectile.

Most efforts to include core excitation in the reaction model have been performed in a static way. For example in [173, 174], core excitation components of the initial wavefunction are included in a DWBA calculation for the Coulomb dissociation of the ^{11}Be, ^{17}C and ^{19}C. Yet there is no dynamical excitation of the core throughout the reaction process. In other words, core excitation could not be generated in the reaction. This approximation does not seem adequate, especially in cases where the couplings to core excited states are strong. The best attempt so far of studying the effect of core excitation in reactions with light exotic nuclei was performed in [137]. In that work, core excitation in ^{8}B was dynamically included in the transfer reaction ^{14}N(^{7}Be,^{8}B)^{13}C. A CDCC-BA formalism was used, employing the approximation that the continuum bin-states could still be described within a single particle picture [137]. As a conclusion of that work, core excitation turned out not to be important. One should note that there is an inconsistency in the calculation [137] in that the projectile Hamiltonian for the bound state is not the same as that for the unbound states. There are non-orthogonality issues that arise and should be investigated. Further work on generalizing CDCC with core excited bins is underway.

Recent results show that, as one moves away from the stability line, few-body models are less successful. An example can be found in [175] where many ^{12}Be reaction observables are compared with recent data. The three body model of ^{10}Be+n+n in which the core ^{10}Be is assumed to be a perfect rotor and is allowed to excite to the first 2^+ state, is unable to reproduce the correct E2 transition $2^+ \rightarrow 0^+$ for ^{12}Be, if all other observables are to be reproduced. This suggests that the simple core excitation ideas need to be revisited. Microscopic information needs to be integrated to an extent that it becomes useful in a reaction model, and yet retains the necessary detail. This balance is one of the most challenging problems to be dealt with in the near future.

10.3. New physics with electron beams

For half a century, electron scattering experiments on nuclei have contributed significantly to our understanding of the structure of stable nuclei. However, since short-lived exotic species cannot form a nuclear target that is at rest in the laboratory frame, electron-nucleus (eA) colliders are being built [176, 177] which will give access to structure studies of unstable nuclei, opening up a new era of low-energy electron scattering. Due to the limited luminosities achieved with radioactive beams, the first generation of experiments with these colliders will focus on measurements of the radii of

the nuclear charge distribution and its diffuseness. Electron scattering on a large variety of unstable nuclei will become possible and will help clarify the evolution of charge radii towards the driplines.

Since the electromagnetic interaction is relatively weak, multiple scattering effects can be neglected in electron scattering and the interaction can be well described by one-photon exchange terms. By combining the charge distributions from electron scattering with matter distributions from hadronic probes such as proton scattering (in inverse kinematics) it will be possible to determine proton and neutron distributions separately for a large number of exotic nuclei.

More interestingly, inelastic electron scattering, which is known to be an excellent tool for studying the spectroscopy of bound and unbound states in nuclei, will also be possible. The transition form factors are related to different multipolarities of the excitations and offer a unique way of studying collective motion in unstable nuclei.

In addition, inclusive quasielastic scattering, $A(e,e')$, is well-known as a way of probing nucleon motion within the nucleus [178]. Exclusive quasielastic scattering involves detecting a knocked-out constituent in coincidence with the electron, $A(e,e'x)B$. For instance, the unpolarized quasifree $(e,e'p)$ reaction has been systematically used to probe single particle properties of complex nuclei, such as momentum distributions and spectroscopic factors. Excellent agreement with experiment has been obtained for these observables for both ^{6}Li$(e,e')^6$Li [179] and ^{7}Li$(e,e'p)^6$He [180] reactions. The reliability of the information extracted from such reactions is due to the weak dependence of the observables upon the electron scattering kinematical conditions. This is particularly true in the quasielastic region, where both the momentum transfer and energy transfer are high enough for the interaction between the electron and a single nucleon in the nucleus to dominate.

Due to the novelty and relatively recent interest in this field, there has been, as yet, very little theoretical work. The only available calculations[181], for electrons scattering from ^{6}He, make use of the plane wave impulse approximation PWIA (which assumes that the virtual photon is absorbed by a single constituent). While that study described the ^{6}He as a three-body system, the authors make several further simplifying assumptions, such as neglecting the Coulomb distortion of the electron, and final state interactions of the knocked out constituent with the spectator constituents. Further work is clearly needed, and on a range of light exotic nuclei.

11. Summary

The relatively new field of the structure and reactions of light exotic and halo nuclei has certainly provided a 'wake up' call for nuclear theorists. Textbook models have been applicable in certain cases while elsewhere new approaches have had to be developed. We stress though that reviews such as this act only as staging posts along the road; there is still a challenging and no doubt fascinating journey ahead.

Acknowledgments

The authors wish to thank Prof. I.J. Thompson for valuable comments on the manuscript. We are grateful to T. Aumann, W. Catford, H. Esbensen, S. Ershov, K. Hagino, P.G. Hansen, N. Timofeyuk and V. Lapoux for kindly providing some of the figures included in the review. The work of J.A-K is supported by the United Kingdom Engineering and Physical Sciences Research Council (EPSRC) through grants GR/M82141 and GR/R78633/01. Support from the Portuguese Science and Technology Foundation under grant POCTI/43421/FNU/2001 is also acknowledged.

[1] I. Tanihata, J. Phys. **G 22** (1996) 157.
[2] P.G. Hansen, A.S. Jensen ad B. Jonson, Ann. Rev. Nucl. Part. Sci. **45** (1995) 591.
[3] N. Orr, Nucl. Phys. **A 616** (1997) 155c.
[4] F.M. Nunes and I.J. Thompson, Modeling of reactions with exotic nuclei, in: Proc. International Nuclear Physics Conference (INPC2001), Berkeley —- August, 2001.
[5] I.J. Thompson and Y. Suzuki, Nucl. Phys. **A 693** (2001) 424.
[6] J.S. Al-Khalili, Eur. Phys. J. A. **15** (2002) 115.
[7] J.S. Al-Khalili, *Nuclear Structure and Dynamics at the Limits*, Ed. H. Feldmeier *et al.*, Proceedings of Int. Workshop XXXI on Gross Properties of Nuclei and Nuclear Excitations, Hirschegg (2003) 176.
[8] I. Tanihata *et al.*, Phys. Rev. Lett. **55** (1985) 2676.
[9] I. Tanihata *et al.*, Phys. Lett. **B 160** (1985) 380.
[10] J.S. Al-Khalili and J.A. Tostevin, Phys. Rev. Lett. **76** (1996) 3903.
[11] J.S. Al-Khalili, J.A. Tostevin and I.J. Thompson Phys. Rev. C **54** (1996) 1843.
[12] N. Austern *et al.*, Phys. Rep. **154** (1987) 125.
[13] J.S. Al-Khalili and J.A. Tostevin, *Scattering*, Ed. P Sabatier and E R Pike, (Academic, London, 2001) Chap. 3.1.3.
[14] I.J. Thompson, Comp. Phys. Rep. **7** (1988) 167.
[15] I.J. Thompson, FRESCO users' manual, University of Surrey, 2000.
[16] J.A. Tostevin, F.M. Nunes and I.J. Thompson, Phys. Rev. **C 63** (2001) 024617.
[17] R.C. Johnson and P.J.R. Soper, Phys. Rev. C **1**, (1970) 976.
[18] R.J. Glauber, in *Lectures in Theoretical Physics*, ed. W.E. Brittin (Interscience, N.Y., 1959) Vol. 1, p. 315.
[19] J.M. Brooke, J.S. Al-Khalili and J.A. Tostevin, Phys. Rev. C **59** (1999) 1560.
[20] G.D. Alkhazov G D, S.L. Belostotsky and A.A. Vorobyov, Phys. Rep. **42** (1974) 89.
[21] R. Serber, Phys. Rev. **72** (1947) 1008.
[22] A. Bonaccorso and D.M. Brink, Phys. Rev. C **57**, (1998) R22.
[23] A. Bonaccorso and D.M. Brink, Phys. Rev. C **58**, (1998) 2864.
[24] A. Bonaccorso, Phys. Rev. **60** (1999) 0546041.
[25] V.S. Melezhik and D. Baye, Phys. Rev. C **59**, (1999) 3232.
[26] P.J. Karol, Phys. Rev. C **11**, (1974) 1203.
[27] R.C. Johnson and C.J. Goebel, Phys. Rev. C **62**, (2000) 027603.
[28] J.S. Al-Khalili *et al.*, Phys. Lett. B **387** (1996) 45.
[29] J.A. Tostevin *et al.*, Phys. Rev. C **56** (1997) R2929.
[30] I.Pecina *et al.*, Phys. Rev. C **52** (1995) 191.
[31] J.J. Kolata *et al.*, Phys. Rev. Lett. **69** (1992) 2631.
[32] M. Lewitowicz *et al.*, Nucl. Phys. **A 562** (1993) 301.
[33] M. Zahar *et al.*, Phys. Rev. C **49** (1994) 1540.
[34] V. Lapoux *et al.*, Phys. Rev. C **66** (2002) 034608.
[35] H. Sagawa, Phys. Lett. B **286** (1992) 7.
[36] G.R. Satchler and W.G. Love, Phys. Rep. **55** (1979) 183.
[37] J.S. Al-Khalili, Nucl. Phys. **A 581** (1995) 315.
[38] J.S. Al-Khalili and J.A. Tostevin, Phys. Rev. C **49** (1994) 386.
[39] K. Rusek and K.W. Kemper, Phys. Rev. C **61** (2000) 034608.
[40] V. Lapoux *et al.*, Phys. Lett. **B 517** (2001) 18.
[41] K. Yabana, Y. Ogawa and Y. Suzuki, Phys. Rev. C **45** (1992) 2909; Nucl. Phys. **A 538** (1992) 295.
[42] J.S. Al-Khalili, I.J. Thompson and J.A. Tostevin, Nucl. Phys. **A 581** (1995) 331.
[43] J.A. Christley, J.S. Al-Khalili, J.A. Tostevin and R.C. Johnson, Nucl. Phys. **A 624** (1997) 275.
[44] J.A. Tostevin *et al.*, Phys. Rev. C **56** (1997) R2929.
[45] M.V. Zhukov, A.A. Korsheninnikov and M. Smedberg, Phys. Rev. C **50** (1994) R1.

[46] G.D. Alkhazov *et al.*, Nucl. Phys. A **712** (2002) 269; S.R. Neumaier *et al.*, Nucl. Phys. A **712** (2002) 247.
[47] J.S.Al-Khalili and J.A. Tostevin, Phys. Rev. C **57** (1998) 1846.
[48] G.D. Alkhazov *et al.*, Phys. Rev. Lett. **78** (1997) 313.
[49] N.C. Summers, J.S. Al-Khalili and R.C. Johnson, Phys. Rev. C **66** (2002) 014614.
[50] R.C. Johnson, J.S. Al-Khalili and J.A. Tostevin, Phys. Rev. Lett. **79** (1997) 2771.
[51] D.T. Khoa, G.R. Satchler and W. von Oertzen, Phys. Rev. C **56** (1997) 954.
[52] R. Crespo and R.C. Johnson, Phys. Rev. C **60** (1999) 034007.
[53] A.K. Kerman, H. McManus and R.M. Thaler, Ann. Phys. (N.Y.) **8** (1959) 551.
[54] R. Crespo and I.J. Thompson, Phys. Rev. C **63** (2001) 044003.
[55] S. Karataglidis *et al*, Phys. Rev. Lett. **79** (1997) 1447.
[56] R. Crespo, I.J. Thompson and A.A. Korsheninnikov, Phys. Rev. C **66** (2002) 021002(R).
[57] P.J. Dortmans and K. Amos, Phys. Rev. C **49** (1994) 1309.
[58] S. Karataglidis *et al*, Phys. Rev. C **52** (1995) 861; Phys. Rev. C **52** (1995) 3224; Phys. Rev. C **53** (1996) 838; Phys. Rev. C **55** (1997) 2826; P.J. Dortmans *et al*, Phys. Rev. C **57** (1998) 2433; Phys. Rev. C **58** (1998) 2249.
[59] A. Lagoyannis *et al*, Phys. Lett. B **518** (2001) 27.
[60] K. Alder, T. Huus, B. Mottelson and A. Winther, Nucl. Phys. **28** (1956) 432.
[61] A. Winther and K. Alder, Nucl. Phys. **A 319** (1979) 518.
[62] G. Baur, C.A. Bertulani and H. Rebel, Nucl. Phys. **A 458** (1986) 188.
[63] G. Baur and H. Rebel, J. Phys. G (1994) 1.
[64] C. Bertulani, Nucl. Phys. **587** (1995) 318.
[65] T. Motobayashi, Phys. Rev. Lett. **73** (1994) 2680.
[66] K. Langanke and T.D. Shoppa, Phys. Rev. **C 49** (1994) R1771.
[67] S. Typel and G. Baur, Phys. Rev. **C 49** (1994) 379.
[68] S. Typel, H. Wolter and G. Baur, Nucl. Phys. **A 613** (1997) 147.
[69] H. Esbensen and G.F. Bertsch, Nucl. Phys. **A 600** (1996) 37.
[70] H. Esbensen, G.F. Bertsch and C.A. Bertulani, Nucl. Phys. **A 581** (1995) 107.
[71] A. Romanelli, L.F. Canto, R. Donangelo and P. Lotti, Nucl Phys. **A 588** (1995) 71c.
[72] C.H. Dasso, S.M. Lenzi and A. Vitturi, Nucl. Phys. A639 (1998) 635; Phys. Rev. **C 59** (1999) 539.
[73] H. Esbensen and G.F. Bertsch, Phy. Rev. **C 59** (1999) 3240.
[74] H. Esbensen and G.F. Bertsch, Nucl. Phys. **A 706** (2001) 383.
[75] M. Fallot, J.A. Scarpaci, D. Lacroix, Ph. Chomaz and J. Margueron, Nucl. Phys. **A 700** (2002) 70.
[76] J. Margueron, A. Bonaccorso and D.M. Brink, Nucl. Phys. **A 703** (2002) 105.
[77] J. Margueron, A. Bonaccorso and D.M. Brink, Nucl. Phys. **A 720** (2003) 337.
[78] T. Nakamura *et al.*, Phys. Rev. Letts. 83 (1999) 1112.
[79] Y. Iwata *et al.*, Phys. Rev. **C 62** (2000) 064311.
[80] T. Kikuchi *et al.*, Phys. Lett. **B 391** (1997) 261.
[81] R. Shyam, I.J. Thompson and A.K. Dutt-Mazumder, Phys. Lett. **B 371** (1996) 1.
[82] R. Shyam and I.J. Thompson, Phys. Rev. **C 59** (1999) 2645.
[83] J. von Schwarzenberg *et al.*, Phys. Rev. **C 53** (1996) R2598.
[84] V. Guimarães *et al.*, Phys. Rev. Lett. **84** (2000) 1862.
[85] J.J. Kolata *et al.*, Phys. Rev. **C 63** (2001) 024616.
[86] F.M. Nunes and I.J. Thompson, Phys. Rev. **C 57** (1998) R2818.
[87] S.N. Ershov, B.V. Danilin and J.S. Vaagen, Phys. Rev. **C 62** (2000) 041001(R).
[88] R. Chatterjee, P. Banerjee and R. Shyam, Nucl. Phys. **A 692** (2001) 476.
[89] M. Yahiro, N. Nakano, Y. Iseri and M. Kamimura, Prog. Theo. Phys. **67** (1982) 1464; Prog. Theo. Phys. Suppl. **89** (1986) 32.
[90] N. Austern, Y. Iseri, M. Kamimura, M. Kawai, G. Rawitscher and M. Yahiro, Phys. Rep. **154**

(1987) 125.
[91] N. Austern, M. Kawai, M. Yahiro, Phys. Rev. **C 53** (1996) 314.
[92] R.A.D. Piyadasa, M. Kawai, M. Kamimura, M. Yahiro, Phys. Rev. **C 690** (1999) 044611.
[93] F.M. Nunes and I.J. Thompson, Phys. Rev. **C 59** (1999) 2652.
[94] J. Mortimer, I.J. Thompson and J.A. Tostevin, Phys. Rev. **C 65** (2002) 064619.
[95] B. Davids *et al.*, Phys. Rev. Lett. **81** (1998) 2209.
[96] B. Davids *et al.*, Phys. Rev. Lett. **86** (2001) 2750.
[97] B. Davids, S.M. Austin, D. Bazin, H. Esbensen, B.M. Sherill, I.J. Thompson and J.A. Tostevin, Phys. Rev. **C 63** (2001) 065806.
[98] G.R. Kelly *et al.*, Phys. Rev. **C 63** (2000) 024601.
[99] E.F. Aguilera *et al.*, Phys. Rev. Lett. **84** (2000) 5058.
[100] J.A. Tostevin, S. Rugmai and R.C. Johnson, Phys. Rev. **C 57** (1998) 3225.
[101] P. Banerjee, J.A. Tostevin and I.J. Thompson, Phys. Rev. **C** (1998) 1337.
[102] D.P. Balamuth *et al.*, Phys. Rev. Lett. **72** (1994) 2355.
[103] E. Alt and A.M. Mukhamedzhanov, Phys. Rev. **C 63** (2001) 044005.
[104] N. Iwasa, Phys. Rev. Lett. **83** (1999) 2910.
[105] E. Garrido, D.V. Fedorov and A. Jensen, Phys. Rev. **C 58** (1998) 2654.
[106] E. Garrido, D.V. Fedorov and A. Jensen, Phys. Rev. **C 59** (1999) 1272.
[107] E. Garrido, D.V. Fedorov and A. Jensen, Nucl. Phys. **A 695** (2001) 109.
[108] E. Garrido, D.V. Fedorov and A. Jensen, Phys. Rev. Letts. **86** (2001) 1986.
[109] T. Kobayashi *et al.*, Phys. Rev. Lett. **60** (1988) 2599.
[110] E. Sauvan *et al.* Phys. Lett. B **491** (2000) 1.
[111] P.G. Hansen, Phys. Rev. Lett. **77** (1996) 1016.
[112] M.M. Obuti *et al*, Nucl. Phys. A **609** (1996) 74.
[113] F. Barranco, E. Vigezzi and R.A. Broglia, Phys. Lett. B **319** (1993) 387.
[114] M. Zinser *et al.*, Phys. Rev. Lett. **75** (1995) 1719.
[115] S.N. Ershov *et al.*, Phys. Rev. Lett. **82** (1999) 908.
[116] M.S. Hussein and K.W. McVoy, Nucl. Phys. **A445** (1985) 124.
[117] F. Barranco, E.Vigezzi and R.A. Broglia, Z. Phys. A **356** (1996) 45.
[118] G.F. Bertsch, K. Hencken and H. Esbensen, Phys. Rev. C **57** (1998) 1366.
[119] J.A. Tostevin, J. Phys. G: Nucl. Part. Phys. **25** (1999) 735.
[120] V. Maddalena *et al.*, Phys. Rev. C **63** (2001) 024613.
[121] J.S. Al-Khalili, Nucl. Phys. **A689**, (2001) 551c.
[122] A. Navin *et al.*, Phys. Rev. Lett. **85** (2000) 266.
[123] F.M. Nunes *et al.*, Nucl. Phys. **A609** (1996) 43.
[124] U. Datta Pramanik *et al.*, Phys. Lett. B **551** (2003) 63.
[125] P.G. Hansen and J.A. Tostevin, Ann. Rev. Nucl. Part. Sci. **53** (2003) xxxx.
[126] G.R. Satchler, Direct Nuclear Reactions, Oxford University Press, 1982.
[127] B.A. Brown, Prog. Part. Nucl. Phys. **47** (2001) 517.
[128] L. Trache *et al.*, Phys. Rev. **C 61** (2000) 024612.
[129] J.C. Fernandes, R. Crespo, F.M. Nunes and I.J. Thompson, Phys. Rev. **C 59** (1999) 2865.
[130] J. Winfield *et al.*, Nucl. Phys. **A 683** (2001) 48.
[131] R. Lewis and A.C. Hayes, Phys. Rev. **C 59** (1999) 1211.
[132] A.M. Mukhamedzhanov *et al.*, Phys. Rev. **C 56** (1997) 1302; H.M. Xu *et al.*, Phys. Rev. Letts. **73** (1994) 2027.
[133] A. Azhari *et al.*, Phys. Rev. Letts. **82** (1999) 3960; Phys. Rev. **C 60** (1999) 055803; Phys. Rev. **C 63** (2001) 055803.
[134] Yu. Oganessian, V.I Zagrebaev and J.S. Vaagen, Phys. Rev. **C 60** (1999) 044605.
[135] F.M. Nunes and A.M. Mukhamedzhanov, Phys. Rev. **C 64** (2001) 062801.
[136] A. Moro, R. Crespo, F.M. Nunes and I.J. Thompson, Phys. Rev. **C 66** (2002) 024612.
[137] A. Moro, R. Crespo, F.M. Nunes and I.J. Thompson, Phys. Rev. **C 67** (2003) 047602.

[138] K. Ogata, M. Yahiro, Y. Iseri, M. Kamimura, Phys. Rev. **C 67** (2003) 011602.
[139] A.N. Ostrowski *et al.*, J. Phys. **G 24** (1998) 1553; G.M. Ter-Akopian *et al.*, Phys. Lett. **B 426** (1998) 251; R. Raabe *et al.*, Phys. Lett. **B 458** (1999) 1.
[140] N.K. Timofeyuk nd I.J. Thompson, Phys. Rev. **C 61** (2000) 044608.
[141] F. Carstoiu, C. Lazard, R.J. Lombard, Phys. Rev. **C 57** (198) 3237.
[142] N.K. Timofeyuk and R.C. Johnson, Phys. Rev. **C 59** (1999) 1545.
[143] A. Moro *et al.*, *submitted to* Phys. Rev. C (2003).
[144] C.Y. Wong, Phys. Rev. Lett. **31** (1973) 766.
[145] R.A. Broglia, C.H. Dasso, S. Landowne and A. Winther, Phys. Rev. **C 27** (1983) 2433.
[146] C.H. Dasso and S. Landowne, Nucl. Phys. **A 405** (1983) 381.
[147] C.H. Dasso, S. Landowne and A. Winther, Nucl. Phys. **A 407** (1983) 221.
[148] S. Landowne and S.C. Pieper, Phys. Rec. **C 29** (1984) 1352.
[149] R. Lindsay and N. Rowley, J. Phys. **G 10** (1984) 805.
[150] I.J. Thompson, M.A. Nagarajan, J.S. Lilley and B.R. Fulton, Phys. Lett. **B 157** (1985) 250.
[151] H. Timmers *et al.*, Nucl. Phys. **A 633** (1998) 421.
[152] N. Alamanos, A. Pakou, V. Lapoux,J.L. Sida and M. Trotta, Phys. Rev. **C 65** (2002) 054606; and references therein.
[153] J. Takahashi *et al.*, Phys. Rev. Lett. **78** (1997) 30.
[154] M.S. Hussein, M.P Pato, L.F. Canto and R. Donangelo, Phys. Rev. **C 46** (1992) 377.
[155] C.H. Dasso and A. Vitturi, Phys. Rev. **C 50** (1994) R12.
[156] M.S. Hussein, M.P Pato, A.F.R. de Toledo de Piza, Phys. Rev. **C 51** (1995) 846.
[157] W. von Oertzen and I. Krouglov, Phys. Rev. **C 53** (1996) R1061.
[158] K. Yabana, Prog. Theo. Phys. **97** (1997) 437.
[159] K. Hagino, A. Vitturi, C. Dasso and S.M. Lenzi, Phys. Rev. **C 61** (2000) 037602.
[160] K. Hagino and A. Vitturi, Proceeding for *Fusion dynamics at the extremes*, Dubna, Russia, May 2000, World Scientific.
[161] A. Diaz-Torres and I.J. Thompson, Phys. Rev. **C 65** (2002) 024606.
[162] F. Brady *et al.*, Phys. Rev. Lett. **51** (1983) 1320.
[163] S. Takeuchi *et al.*, Phys. Lett. B **515** (2001) 255.
[164] T. Nakamura *et al.*, Phys. Lett. B **493** (2000) 209.
[165] S.N. Ershov *et al.*, Phys. Rev. C **56** (1997) 1483.
[166] S. Rugmai, J.S. Al-Khalili, R.C. Johnson and J.A. Tostevin, Phys. Rev. C **60** (2000) 7002.
[167] S. Karataglidis, P.J. Dortmans, K. Amos and C. Bennhold, Phys. Rev. C **61** (2000) 024319.
[168] S. Karataglidis and C. Bennhold, Phys. Rev. Lett. **80** (1998) 1614.
[169] M.J. Boland *et al.*, Phys. Rev. C **64** (2001) 031601(R).
[170] J.A. Tostevin, Nucl. Phys. **A 682** (2001) 320c.
[171] A.M. Moro *et al.*, Phys. Rev. C 65 (2001) 062801.
[172] D. Cortina-Gil *et al.*, Phys. Lett. **B 529** (2002) 36.
[173] V. Maddalena and R. Shyam, Phys. Rev. **C 63** (2001) 051601(R).
[174] R. Shyam and P. Danielewicz, Phys. Rev. **C 63** (2001) 054608.
[175] F.M. Nunes, I.J. Thompson and J.A. Tostevin, Nucl. Phys. **A 703** (2002) 593
[176] *An International Accelerator Facility for Beams of Ions and Antiprotons*, GSI Report, 2002 (http://www.gsi.de/GSI-Future/cdr/).
[177] T. Suda and K. Maruayama, Proposal for RIKEN Beam Factory, RIKEN, 2001.
[178] T.W. Donnelly and A.S. Raskin, Ann. Phys. (N.Y.) **169** (1986) 247.
[179] R.B. Wiringa and R. Schiavilla, Phys. Rev. Lett. **81** (1998) 4317.
[180] L.Lapikás, J. Wesseling and R.B. Wiringa, Phys. Rev. Lett. **82** (1999) 4404.
[181] E. Garrido and E. Moya de Guerra, Nucl. Phys. A **650** (1999) 387.